ISSN 2310-5607

PREMIER Publishing

# Austrian Journal of Technical and Natural Sciences

Premier Publishing s.r.o.

2023
5-6

# Austrian Journal of Technical and Natural Sciences

№ 5–6 2023
May– June

PREMIER
Publishing

Vienna
2023

# Austrian Journal of Technical and Natural Sciences

Scientific journal

№ 5–6 2023 (May– June)

ISSN 2310-5607



**Proofreading** Kristin Theissen

**Cover design** Andreas Vogel

**Additional design** Stephan Friedman

**Editorial office** Premier Publishing
Praha 8 – Karlín, Lyčkovo nám. 508/7, PSČ 18600

**E-mail:** pub@ppublishing.org

**Homepage:** ppublishing.org

**Austrian Journal of Technical and Natural Sciences** is an international, German/English/Russian language, peer-reviewed journal. The journal is published in electronic form.

The decisive criterion for accepting a manuscript for publication is scientific quality. All research articles published in this journal have undergone a rigorous peer review. Based on initial screening by the editors, each paper is anonymized and reviewed by at least two anonymous referees. Recommending the articles for publishing, the reviewers confirm that in their opinion the submitted article contains important or new scientific results.

Premier Publishing is not responsible for the stylistic content of the article. The responsibility for the stylistic content lies on an author of an article.

Instructions for authors

Full instructions for manuscript preparation and submission can be found through the Premier Publishing home page at:
http://ppublishing.org.

Material disclaimer

The opinions expressed in the conference proceedings do not necessarily reflect those of the Premier Publishing, the editor, the editorial board, or the organization to which the authors are affiliated.

Premier Publishing is not responsible for the stylistic content of the article. The responsibility for the stylistic content lies on an author of an article.

Included to the open access repositories:


SJIF 2023 = 5.859 (Scientific Journal Impact Factor Value for 2023).


Included to the Uzbekistan OAK journals bulletin.



Typeset in Berling by Ziegler Buchdruckerei, Linz, Austria.
Printed by Premier Publishing, Vienna, Austria on acid-free paper.

# Section 1. Biotechnologies

**https://doi.org/10.29013/AJT-23-5.6-3-9**

*Martirosyan Hamlet Sargisovich,*
*Associate Professor, Department of Plant Growing and Soil Science,*
*Armenian National Agrarian University, Yerevan, Armenia*

*Avetisyan Arevhat Semyonovna,*
*Vice Dean for Academic Affairs of the Faculty of Biology,*
*Chemistry and Geography,*
*Laboratory of the Scientific Laboratory for the study*
*of Biologically Active Compounds and Biosafety,*
*Armenian State Pedagogical University*
*Named after Kh. Abovyan, Yerevan, Armenia*

*Sadoyan Ruzanna Robertovna,*
*Doctor of Biological Sciences,*
*Dean of the Faculty of Biology, Chemistry and Geography,*
*Armenian State Pedagogical University*
*Named after Kh. Abovyan, Yerevan, Armenia*

## WAYS OF OBTAINING ORGANIC PRODUCTS FROM SEVERAL BREAD CROPS (BARLEY, EMMER AND WHEAT)

**Abstract.** With the aim of effective cultivation of cereal crops and obtaining organic products, the effect of ecologically safe preparations on the quantity and quality of the yield of several bread crops was studied. Our results showed that investigated preparations can be recommended as a new effective and safe agrochemical for crop cultivation.

**Keywords:** Organic preparation, seed disinfectant, Complex-Co, Bactophyte, Quicelium, Triamin 10.2%, growth stimulant, barley, emmer, triticale.

**Introduction**

To solve the food problem, meet the growing needs of the population for food and provide livestock feed, it is extremely important to obtain new, highly productive varieties of agricultural crops that can best withstand the stressful situations observed as a result of global climate change [1, 111; 2, 328; 3, 203–209]. In this way, it is no less important and very responsible process to develop a complex of scientifically based agrotechnical measures for newly obtained and high-efficiency varieties, under which conditions the variety can demonstrate its potential possibilities of efficiency. Here, in particular, great attention should be paid to the definition of the exact fertilization system, choosing the optimal combination of fertilizers, on which both the quantity and

quality of the expected harvest largely depend [4, 114–119; 5].

In modern conditions, it is becoming very relevant to obtain an environmentally pure product, which is free from unwanted compounds harmful to human health and residual nitrogen. In this regard, bread crops are extremely important, the products obtained from which are a daily component of the human diet [6]. It is equally important to pay similar attention to the quality indicators of grain feed used in the ration of farm animals, because in order to obtain high-quality livestock products, it is necessary to feed animals with quality feed without extraneous additives [7; 8]. The solution to this global problem should start from the very initial stage of crop cultivation, seed disinfection, continuing it throughout the vegetation and excluding the use of any mineral fertilizers in the form of nutrients. For this purpose, we used "Complex – Co" preparation of organic origin as a seed disinfectant, which is a highly effective means of combating bread crops against fungal diseases [9, 285–290]. At the same time, it also has the best properties of a plant growth promoter, significantly increasing the degree of effective plant tillering in bread crops. The above mentioned valuable properties of "Complex – Co" organic preparation were presented in our previous report [10].

**Material and method**

This time, the order and sequence of organic fertilizers used during the subsequent stages of the cultivation of several spiked bread crops (barley, emmer, wheat) obtained by us are presented, as well as the effect of fertilizers on the chemical composition of the grain and the main provisions for obtaining an ecologically clean product [11; 12, 413; 13, 175].

At the early stage of plant growth and development (stemming and spring regrowth) on the background of "Comlex-Co" preparation, Triamin 10.2% organic fertilizer given in the form of extra-root nutrition had a significant effect. It is a liquid fertilizer containing amino acids and microelements, which is applied to a number of agricultural crops, particularly bread crops. The preparation is developed specifically for the stimulation of plant growth and the formation of new tissues, significantly contributes to the improvement of the plant's immune system, increasing resistance to diseases. At the same time, it provides the plant with microelements necessary for growth [14, 72–79; 15, 702–707].

In the later stages of the growth and development of bread crops, the fight against fungal diseases (downy mildew and leaf rust) was carried out with Bactophyt biological fungicide preparation, at the beginning of the tube setting stage. It is a biological fungicide and bactericide preparation for grain, fruit and vegetable crops to combat fungal and bacterial diseases. At the same time, the preparation provides a good result in the fight against root rot, powdery mildew, rust and fusarium.

The application of organic fertilizer Quiselium, which is applied in the form of extra-root nutrition at the end of the flowering of bread crops, as soon as grain formation begins, provides a noticeable increase in the grain yield of bread crops. It is a liquid fertilizer containing microelements derived from valuable plant extracts. The preparation stimulates the division of cells, the process of plant growth, which in the end noticeably increases the yield and increases the sugar content.

Each of the selected preparations has its own specific mechanism of action and period of application, which determines the level of effectiveness of the given preparation. For this reason, when conducting scientific experiments, a very stable schedule for the use of organic preparations was defined, because each of them can provide its maximum result in a very specific period of time and at the planned stage of growth and development [16, 71–75;17, 422].

All three preparations used during the vegetation has organic origin, as a result of their after-effect, obtaining an ecologically pure product is fully guaranteed. Here it is also worth mentioning the fact that the soils of the test field, where the scientific experiments were carried out, are certified by the "Ecoglobe" organization operating in RA, where no pesticides and mineral fertilizers have been used

for more than ten years [18,112]. At the end of the three-year studies, average samples were separated from the product (grain mass) for laboratory examination and determination of the amount of undesirable compounds and residual nitrogen in them. It was carried out in the "FDI" laboratory located in the Abovyan region of the Kotayk marz of RA and having state certification, the results of which are attached to the article in the form of an appendix.

**Results and discussions**

During the cultivation of cereal crops, the use of preparations of organic origin began with the disinfection of seeds, and the effect of the Comlex-Co preparation as a disinfectant and growth promoter on seed germination capacity and duration was studied.

Organic fertilizer of Triamin 10.2% introduced in the form of foliar feeding had a significant effect on the background of Comlex-Co preparation in the early stage of plant growth and development (tillering and spring regrowth). This is evidenced by the indicators of productive tillering introduced in Table 1, which significantly exceed the results of the control variant.

The highest rate of productive tillering was observed in barley – 1.31, which exceeded the control option of the same crop by 0.21, while in emmer and triticale, these differences compared to the control one were 0.12 and 0.15, respectively.

Triamin 10.2% preparation applied in the form of foliar feeding during vegetation had a noticeable effect on the number of total stems, as well as stems with spike, which is one of the primary and important prerequisites for the formation of high grain yield. The increase in the number of cereal crop total stems in the variants treated with the preparations can be attributed mainly to the aftereffect of the Complex-Co preparation, and later the intensive rate of their growth may be related to the Triamin 10.2% organic preparation. At the early growing stage Complex-Co promotes the intensive accumulation of nutrients in the tillering node, which in its turn leads to the formation of a large number of stems. It is especially well manifested in the case of triticale, increasing the number of stems with spike by 75.1 units compared to the control variant, and in the case of barley and emmer, it was 42.6 and 10.8 stems, respectively.

At the early stages of growth and development, the formation of healthy plants and their high level of preservation is provided by the Complex-Co preparation, and during the vegetation period, the application of Bactophyte organic preparation in the form of foliar feeding, which had a significant effect on the prevention of diseases characteristic to the cereal crops. This is evidenced by the phytopathological data presented in Table 2, which clearly state that in all the crops of the variants fertilized with organic fertilizers, the infection intensity with diseases was assessed with a of 5 ball. An exception was observed in case of emmer, where a few traces of leaf rust was recorded and due to that it was scored as 4.9 ball and this was during the summer season with high amount of precipitations.

Table 1.– Effect of organic fertilizers on stem extension capacity of spiked cereals

| Crop | Variant | Number of stems per 1 $m^2$, unit | | Tillering | | Plant height by stages, cm | | | | The intensity of the infection of the plants with diseases, ball |
|---|---|---|---|---|---|---|---|---|---|---|
| | | total | with spike | total | productive tillering | tillering | stem extension | heading | ripening | |
| *1* | *2* | *3* | *4* | *5* | *6* | *7* | *8* | *9* | *10* | *11* |
| Barley | Control | 646.5 | 467.8 | 1.52 | 1.10 | 13.1 | 41.3 | 66.1 | 71.8 | 4.9 |
| | Treated with preparations | 878.6 | 510.4 | 1.91 | 1.31 | 16.8 | 53.4 | 80.0 | 88.5 | 5.0 |

| *1* | *2* | *3* | *4* | *5* | *6* | *7* | *8* | *9* | *10* | *11* |
|---|---|---|---|---|---|---|---|---|---|---|
| Emmer | Control | 571.1 | 412.7 | 1.55 | 1.12 | 12.1 | 44.7 | 59.8 | 65.0 | 4.5 |
| | Treated with preparations | 688.1 | 423.5 | 1.81 | 1.24 | 14.8 | 52.4 | 68.4 | 72.1 | 4.9 |
| Triticale | Control | 587.3 | 429.3 | 1.45 | 1.05 | 17.8 | 102.3 | 150.3 | 162.7 | 4.8 |
| | Treated with preparations | 790.3 | 504.4 | 1.88 | 1.20 | 20.2 | 114.7 | 189.78 | 197.8 | 5.0 |

The significant positive effect of bactophyte is also testified by the fact that in the control variants of cereal crops, a relatively high level of infection was observed, reaching 4.5–4.9 ball, while it decreased sharply in the variants where preparations were applied.

In the grain formation and filling stages the foliar feeding of plants with Quicelium preparation had its considerable effect on the structural elements of the spike, on the mass of 1000 grains, as well as on the developed biological and actual yield quantity, the results of which are summed up in the Tables 2 and 3.

Table 2. – The effect of organic fertilizers on the biological yield of grain and its structural elements

| **Crop** | **Variant** | **The number of plants per 1 m² at the end of vegetation, unit** | **The number of the stems with spike per 1m², unit** | **One spike** | | | **Weight of 1000 grains, g total** | **Grain yield from 1m², g** | **Biological yield, t/ha** | | |
|---|---|---|---|---|---|---|---|---|---|---|---|
| | | | | **length, cm** | **the number of spikelets, pcs** | **weight of grains, g** | | | **total** | **of which** | |
| | | | | | | | | | | **grain** | **thatch** |
| Barley | control | 425.3 | 467.8 | 6.8 | 34.7 | 0.84 | 38.8 | 392.5 | 89.0 | 39.2 | 49.8 |
| | treated with preparations | 466.4 | 510.4 | 7.4 | 36.8 | 0.88 | 38.4 | 433.3 | 100.5 | 43.7 | 56.8 |
| Emmer | control | 368.5 | 412.7 | 7.0 | 30.7 | 0.71 | 34.8 | 294.7 | 68.5 | 29.8 | 38.7 |
| | treated with preparations | 380.2 | 423.5 | 7.9 | 34.8 | 0.76 | 35.1 | 317.4 | 72.1 | 31.3 | 40.8 |
| Triticale | control | 405.1 | 429.3 | 9.4 | 31.7 | 1.2 | 52.3 | 511.3 | 119.3 | 51.8 | 67.5 |
| | treated with preparations | 420.4 | 504.4 | 10.9 | 39.5 | 1.3 | 52.8 | 674.1 | 156.3 | 67.8 | 88.5 |

The study of data in (Table 2), makes it clear that the applied agro-measures had their effect on the preservation level of the plants at the end of vegetation. From this point of view, particularly barley was distinguished, in case of which the number of preserved plants per unit area ($1m^2$) exceeded the indices of control variant by 41.1, whereas in the emmer and triticale variants it was 11.7 and 15.3 plants, respectively.

The actual amount of grain and thatch yield obtained was determined by the yield amount obtained from the entire experimental bed, based on which the surplus of grain yield (in centner/ha and%) against the control variants was calculated. The highest surplus in actual grain yield was observed for triticale, making 12.7 centner/ha or 30.6%, and for barley and emmer it was 3.3 centner/ha or 10.4% and 3.5 centner/ha or 14.6%, respectively.

Table 3.– Effect of organic fertilizers on grain yield

| Crop | Variant | Yield, centner/ha | | | Yield difference comparing with control | |
|---|---|---|---|---|---|---|
| | | total | of which | | centner/ha | % |
| | | | grain | thatch | | |
| Barley | control | 72.9 | 31.7 | 41.2 | – | – |
| | treated with preparations | 80.5 | 35.0 | 45.5 | 3.3 | 10.4 |
| | $LSD_{05}$ | 8.7 | 7.6 | 7.8 | 1.4 | |
| Emmer | control | 52.6 | 23.9 | 28.7 | – | – |
| | treated with preparations | 60.1 | 27.4 | 32.7 | 3.5 | 14.6 |
| | $LSD_{05}$ | 9.7 | 8.4 | 7.1 | 1.6 | |
| Triticale | control | 95.4 | 41.5 | 53.9 | – | – |
| | treated with preparations | 124.7 | 54.2 | 70.5 | 12.7 | 30.6 |
| | $LSD_{05}$ | 11.0 | 5.2 | 7.1 | 1.9 | |

As a result of the conducted comprehensive studies, it becomes clear that the grain yield of spiked cereal crops obtained by our research group in case of using preparations of organic origin is 2.1–3.4 centner/ha more than when fertilizing the same varieties with accepted doses of mineral fertilizers.

Here it is also necessary to mention the fact that though the quantity of grain yield is of primary importance, the quality of the obtained product is of no less importance, taking into account the amount of residual nitrogen present in its composition. Since the investigated cereals have food (emmer) and fodder (barley, triticale) significance, in both cases the acquisition of ecologically clean product is of high priority. In the latter case the grain comes forth as one of the main components of the animal feed ration, which greatly promotes the manufacture of high quality and eco-livestock product. For this purpose, an average sample was isolated from the grain yield obtained as a result of scientific experiments and subjected to laboratory examination to find out the chemical composition of the grain, emphasizing the amount of harmful nitrogen (residual nitrates) present in it, the results of which are introduced in Table 4. The laboratory examinations were carried out in the "FDA" laboratory of Abovyan province of Kotayk marz.

Table 4.– The effect of organic fertilizers on the chemical composition of grain

| Crop | Variant | Proteins,% | Carbohydrates,% | Nitrate residues, mg/kg |
|---|---|---|---|---|
| Barley | control | 10.1 | 68.8 | 11.1 |
| | treated with preparations | 11.8 | 72.2 | 5.1 |
| Emmer | control | 10.2 | 71.8 | 12.4 |
| | treated with preparations | 11.7 | 79.4 | 4.1 |
| Triticale | control | 9.9 | 77.8 | 10.9 |
| | treated with preparations | 10.8 | 81.9 | 7.8 |

The energy value of food used for both food and feed purposes is first of all estimated based on the percentage content of proteins and carbohydrates present therein. In this regard, when using again organic fertilizers, according to the results of chemical analysis, considerable increase in the amount of those substances was observed in the grain composition. Thus, the protein percentage in the grains of the fertilized variants of the tested cereal crops increased by 0.9–1.5%, and carbohydrates – by 3.4–4.1%, compared to

the control variants of the same crops. Here the issue related to the production of ecologically safe food and fodder is highly important, which is determined by the amount of their nitrate content. In this regard, it should be noted that a certain amount of residual nitrogen was observed in the grain yield obtained from the control variants cultivated in the traditional way, which significantly exceeded the same indicators of the variants cultivated with organic fertilizers. Thus, the amount of residual nitrates in the experimented variants crossed the minimum limit, reaching 4.1–7.8 mg/kg, which was 4.6–6.8 mg/kg lower than the indicators of the control variants. Thus, the results of multi-year studies confirm that organic fertilizers not only greatly increase the amount of grain yield, but also significantly improve the yield quality, making it ecologically safe and harmless to human and animal health. That is why, currently the application of such systems is highly emphasized, which is very efficient and rather prospective in the coming future.

## References:


1. Leontiev M. S., Ovsyannikov Yu. A.– The concept of ensuring food security of the Sverdlovsk region population for the period up to 2015.– 111 p.
2. Astakhov A. S. Ecological safety and efficiency of nature management – Vologda: Infra-Engineering, 2009.– 328 p. URL: http://www.ecocommunity.ru/material.php?id=441
3. Nazarkova-Babkina Yu. D. Environmentally friendly products: challenges and prospects. International scientific journal "bulletin of science".– No. 10 (43).– Vol. 4. 2021.– P. 203–209.
4. Geiger E. Yu., Varlamova L. D., Semenov V. V., Pogodina Yu. V., Sirotina Yu. A. Chelated Microfertilizers: Experience and Prospects for Use, Agrochemical Bulletin, – No. 2. 2017.– P. 114–119.
5. The Food safety inspection body of the Republic of Armenia. URL: https://www.snund.am/hy/page/phytosanitary/102
6. "About the food safety". URL: https://hetq.am/hy/article/130991/ URL: https://hetq.am/hy/article/130991
7. Ra law on organic agriculture.URL: https://www.arlis.am/DocumentView.aspx.DocID=75260
8. Ecology, nature conservation and environmental safety / Ed. V. I. Danilova-Danilyana,. 2 book.
9. Babayan B. G., Mikaelyan A. R., Melkumyan M. A., Bagdasaryan S. A., Grigoryan A. M. Tartaric Acid Synthetic Derivatives for Multi-Drug Resistant Phytopathogen Pseudomonas and Xanthomonas Combating, Science and Technology Publishing,– 4(5). 2020.– P. 285–290.
10. Bella G. Babayan, Aram R. Mikaelyan, Nona L. Asatryan, Marina A. Melkumyan, Samvel A. Bagdasaryan, Anna M. Grigoryan Tartaric Acid New Synthetic Derivatives Antibacterial Activity against the Phytopathogenic Pseudomonas syringae, 2nd International Conference on Advanced Research in Science, Engineering, and Technology (ICARSET), Mar 26–28, 2019. – Paris, France.
11. Martirosyan H. S., Hovhannisyan M. C., Abovvan M. G. // Evaluating the efficiency and resistance towards the abiotic factors in the newly bred varieties of the cereal crops / International journalAgriculture and envoronmental research, 2020.– 1, 9 p.
12. Mineev V. G. Biological farming and mineral fertilizers.– M.: Kolos, 1993.– 413p. (In Russian).
13. Kipriyanov N. A. Environmentally friendly plant raw materials and finished food products.– M., Agar, 1997.– 175 p. (In Russian).
14. Abdelhameed R. M., Abdelhameed R. E., Kamel H. A., 2019. Iron-based metal-organicframeworks as fertilizers for hydroponically grown Phaseolus vulgaris. Mater. Lett.– 237.– P. 72–79.

15. Mikaelyan A. R., Babayan B. G., Asatryan N. L., Vardanyan A. S., Amyan A. M., Nazaretyan A. Kh. The investigating of the Plant Growth stimulator on the bases of Natural Tartaric Acid, NPUA Bulletin, Collection of Scientific Papers,– Vol. 2. 2019.– P. 702–707.
16. Vavilov N. I.– Crop production,– M., Kolos, 1983.– P. 71–75.
17. Dospehov B. A. Field experiment mthodology.– M.– Kolos. 1965 (1985).– 422 p. URL: https://studfile.net/preview/5051840
18. Anderson W. and Smith R. Yield advantage of two semidwarf compared with. 2010.– 112p.

# Section 2. Food processing industry

**https://doi.org/10.29013/AJT-23-5.6-10-13**

*Giyasov Javlonbek Shavkatovich,*
*Doctoral student*
*at Tashkent Chemical-Technological Institute*

## RESEARCH THEORY OF PERIODIC AND CONTINUOUS REFINING PROCESSES

**Abstract.** The disadvantage of the periodic method, used in the oil industry today, is that a long impregnation time is required, the alkali softens the neutral oil, and the amount of neutral oil in the soapstock increases. To overcome these disadvantages, continuous refining is recommended in this research work. In the continuous refining process, neutralization is carried out in special blenders, and the soapstocks are separated in centrifuges. This method reduces the consumption of neutral oil due to the short residence time in the process and the mutual contact of oil and alkali.

**Keywords:** periodic method, continuous method, alkali, centrifuge, soapstock, adsorbent, fatty acid.

The aim of processing fats for food use is to maximise the preservation of the nutritional and physiological value of the oil, without changing the glyceride part of the oil. The conditions of the individual stages of the multi-stage processing process are such that the glyceride part of the oil must not be exposed to strong effects of oxygen, heat and other technological factors. It is characterised by the presence of substances that influence the non-glycerine part of the oil, especially the appearance of the product and the subsequent refining stages [1].

Most of these substances are natural companions of oil triglycerides, while others, on the contrary, are added to the oil during production and at specific processing steps. Natural companions include phosphatides, fatty acids, pigments, various volatiles, and other substances produced during the biosynthetic processes that occur during the growth and ripening of oil crops. Such substances can be used in industry, so they must be extracted from the oil in its natural state while retaining their useful biological or technological properties in the refining process [2].

It should be noted that these substances, namely triglycerides, can undergo significant changes during seed and black oil refining, which can significantly affect the efficiency of the refining methods used. In oil refining, among the substances added to the oil may be moisture, soap residues, requiring auxiliary operations (washing, drying, etc.) [3].

The processing of fats takes place in several stages, as we mentioned above. The processes in these stages are carried out in two different ways: the periodic method and the continuous method.

When using these two methods in the oil industry, we can see that they have their own pros and cons. Let's look at each step in order so that we can understand the difference between the two methods.

**Neutralisation process.** Periodic neutralisation of oils consists of the following consecutive (in time)

processes: formation of soap structures, their formation by coagulation and deposition.

The interaction of free fatty acids with alkali is instantaneous. The time of exposure of the alkali to the oil causes soapy structures to form [4].

The higher the concentration of the aqueous alkaline solution, the greater their ability to saponify free fatty acids. As the concentration of the alkaline solution increases, the diffusion potential of the alkali into the soap structures increases.

The separation (sedimentation) of soapstock and oil in the sedimentation process, which is a long process, practically follows Stokes' law for polydisperse systems. Soapstone settling proceeds under complex conditions of soap briquetting, decomposition and parallel chemical-colloid processes.

The transition to continuous neutralisation leads to a major change in the structure of the soaps, which is primarily due to the speed (time) of the individual stages of the process.

In the continuous neutralization process, as in the periodic process, the formation of a pellicle on the alkali droplet takes place. However, while in the periodic method pellicle formation takes a long time, in the continuous method this process lasts for a short time, i.e. from the time the alkali is added to the oil to the time of splitting in the separator.

The short contact time between the alkali and the oil is sufficient to neutralize the free fat acids, but not sufficient to saponify the neutral oil. Therefore, the neutral oil is saponified to a lesser extent during continuous neutralization.

Neutralization of black cottonseed oil is carried out under more difficult conditions than other oils. For example, the emulsion neutralization of cotton oil using the All-Russia Research and Development Institute of Fats (ARDIF) method has to deal with two soap antagonists, hydrophilic emulsifiers and gossypol, which have a negative effect on emulsification [5].

The pellicle formed on the surface of the alkali droplets at the start of the neutralization process partially adsorbs gossypol and gossypol derivatives (which have not completely lost their polar properties). The result is a homogeneous system in which the soap is distributed between the oil and the alkaline solution.

When water is added, the volume of the aqueous phase increases, which in turn causes a phase change and a break in the oil-saponification bond, i.e. separation of the system.

In the continuous neutralization of black cotton oil, the effect of gossypol and its derivatives on the stability of the system or the duration of the presence of pellicles on the oil surface must be considered. This process tells us that the behavior of toluene droplets and the concentration (composition) of the soap in the aqueous alkaline solution depend on the residence time of the droplet on the oil surface, as shown by Rebinder and Wenström [1].

Table 1.

| **Concentration of soap in millimoles per 1 l** | **Duration of "life" of the droplet on the surface (in seconds)** | |
|---|---|---|
| | **Concentration of soap** | **Toluene** |
| 0 | 0 | 0 |
| 0.025 | 0 | 2 |
| 0.05 | 0 | 47 |
| 0.1 | 1.5 | 28 |
| 0.5 | 2.0 | 95 |
| 2.5 | 5.0 | 223 |
| 5.0 | 7.0 | 480 |
| 10.0 | 12.0 | 1200–1800 |

The data in Table 1 show that the stability of the pellicles increases with increasing soap concentration. In the presence of products of phenolic nature in the oils, it increases even more.

The continuous neutralization process consists of the following successive high-speed processes: heating, dosing, mixing of oil and alkali, and separation of the soapstock.

**Cleaning (washing) soap residue.** The continuous separation of soap residue from the neutralised oil depends on the speed and complete dissolution in water or water-salt solution.

The amount of water required is determined by the soap content of the oil and the nature of the accompanying substances in the oil.

Thus, the accumulation of fat acids, iron and nickel salts should therefore first be removed by exposure to weak saline solutions or by treatment with a water condensate solution.

Normally, the amount of water required in the continuous oil washing process is 10–15% of the weight of the oil. This creates conditions for the molecular solubility of soap in water [2].

In a periodic process, the duration of the oil wash is determined by the time taken to mix the soap phase, dissolve by diffusion and separate the sludge. In a continuous process, time is spent only on soap melting and the separation of the sludge in a continuous mode.

Temperature is an important factor not only for separation systems, but also for ensuring that the soap dissolves completely in the water or water-salt solution. The higher the water and oil temperature, the more completely the soap dissolves in the water. As far as a continuous process is concerned, the optimum temperature is in the 90–950 °C range. A drop in the temperature of the oil or water drastically degrades the washing quality and requires repeated washes, sometimes resulting in the formation of emulsions [4].

The washing process in the continuous method is carried out in the following sequence: heating to optimum temperature, dosing, mixing and separating oil and water.

**Removal of moisture from the oil composition (drying).** No matter how long the sedimentation process lasts, no matter how many attempts are made to separate it in plate or tube centrifuges, it is not possible to completely eliminate the moisture in the water used to wash the soap residue. In the absence of any humectants or stabilisers, some amount of moisture (0.2–1% of the total oil mass) is always retained in a finely dispersed state [5].

The most common method of removing this moisture is vacuum drying. Continuous vacuum drying is based on the evaporation of moisture from the surface of a single drop of oil entering the vacuum dryer.

For efficient fat drying, the batch machine uses intensive mechanical agitators to help push the moist oil droplets upwards. In continuous drying, the same effect is achieved by continuously heating the oil in a vacuum. Oil heated to 35–950 °C is sent to a vacuum chamber, where the moisture is immediately separated from the oil, and the separated moisture is discharged into a condenser. The dried fat droplets collect at the bottom of the vacuum dryer column and are continuously removed [2].

**Cleaning of dyes (bleaching).** The change from periodic to continuous oil bleaching does not involve a change in the adsorption mechanism. The greatest difficulty arises from the need for continuous separation of the adsorbent from the oil.

With continuous bleaching, the mixing time of the oil and adsorbent is maintained. This process can be carried out in contact mixing machines, where a measured amount of oil and adsorbent is premixed and sent to the machine. The mixing time is determined by the nature of the adsorbent and the colouring pigments of the oil and can range from 15 to 45 minutes [6].

A continuous scheme for bleaching oil with solid adsorbents includes the following sequential processes: heating oil, weighing oil and adsorbent, mixing oil and adsorbent, separating adsorbent.

**Cleansing of taste and odour imparting substances (deodorisation).** Despite the obvious

advantages of this method, continuous deodorisation of oil is still not used in some plants.

The most important advantage of continuous deodorisation, which distinguishes it from intermittent deodorisation, is a constant vacuum and temperature.

The continuous deodorisation process creates a constantly reproducible environment for each particle of deodorisable oil, where each drop of oil is always exposed to the same high vacuum and temperature.

Schematically, deodorisation consists of the following processes: continuous heating of de-aerated oil, deodorisation in small layers, continuous heating with dry steam, separation of flavouring and odorous substances and partial free fatty acids, and cooling to a certain temperature.

**Conclusion.** The periodic neutralization method is currently used to treat moderate amounts of oil. This method is carried out in neutralizers with capacities of 5, 10, and 20 tons. The disadvantage of the periodic method is that this process requires a long soaking time, as this process lasts a long time, the lye softens the neutral oil, which increases the amount of neutral oil in the soapstock as a result. Soapstock has a fat content of 30–50%.

In the continuous neutralisation method, the most efficient method is to separate the neutral oil soapstick phases in the field of centrifugal force. In this case the neutralisation is carried out in special mixers and the separation of the soapstocks is carried out in centrifuges. The advantage of this method is the short time needed for the process and the fact that oil and alkali are in short contact with each other, the oil consumption is neutral and the oil content of the soapstock is at a standard level.

## References:

1. Qodirov Y. Yog'larni qayta ishlash texnologiyasi.– T.: "Fan va texnologiya", 2014.
2. Shmidt A. A. "Teoreticheskiye osnovi rafinatsii rastitelnix masel".– M.: Pishevaya promishlennost, 1967.
3. Arutyunyan M. S., Kornena YE. P., Yanova L. I. "Texnologiya pererabotki jirov".– M.: Pishevaya promishlennost, 1970.
4. Vasilyeva G. F., "Dezodoratsiya v maslojirovoy promishlennosti" – M.: Stroypishemash, 2003.
5. Kaloshin Y. A. 'Texnologiya i oborudovaniye maslojirovix predpriyatiy".– M.: Akademiya, 2002.
6. Strijenok A. A. Sovershenstvovaniye texnologii adsorbsionnoy rafinatsii rastitelnix masel, avtoref. diss, kond. texn. nauk 03.06.2015 / A. A. Strijenok Krasnodar, 2015.

# Section 3. Technical sciences in general

**https://doi.org/10.29013/AJT-23-5.6-14-19**

*Kobilov Nodirbek,*
*Khamidov Basit,*
*Shukurov Abror,*
*Kodirov Sarvar,*
*Khidirov Muso,*
*Shukhratov Jahongir,*
*Institute of General and Inorganic Chemistry of Uzbekistan Academy of Sciences*

## INVESTIGATION OF PHYSICAL CHEMICAL PROPERTIES OF DRILLING FLUIDS FOR DRILLING OIL AND GAS WELLS

**Abstract.** The objective of this work is investigation of physical and chemical properties and development new receipt of weighted drilling fluids for drilling oil and gas wells. In the article the main physical and chemical properties of the weighted drilling fluids for drilling oil and gas wells have been given. The methods of testing drilling fluids and materials used for obtaining weighted drilling fluids have been investigated.

**Keywords:** drilling fluid, properties, test, standards, weighting, receipt, well, oil and gas.

**Introduction**

The properties of drilling fluids play important role for oil and gas well drilling. Drilling fluid density is usually called mud weight. Normal pressure formations generally have a pressure gradient similar to a water gradient. For various reasons formation fluid pressures are frequently higher. Barite or hematite is used to increase the drilling fluid density. This increases the hydrostatic gradient in the well bore so that the pressure in the well bore is higher than formation pressure [1; 2].

The most essential properties of drilling fluids are viscosity, mud weight or density, filter cake, Solid's content, gel strength toxicity, fluid rheology, fluid loss, particle plugging, high-angle sag and dynamic high-angle sag, high-temperature fluid aging, cuttings erosion, shale stability, capillary suction time (CST), return permeability, X-ray diffraction and particle-size distribution (PSD).

**Materials and methods**

As a material for obtaining drilling fluids used water, bentonite, carboxymethyl cellulose, gossypol resin, barite ($BaSO_4$) and NaOH, $Na_2CO_3$. Investigations of drilling fluids properties carried out according API (API RP 13-$B_1$, $B_2$) standards. The viscosity is defined as the resistance of fluid to flow. The concepts of viscosity, shear stress, and shear rate are important in understanding the flow characteristics of fluids. Specific measurements are made on fluids to determine rheological parameters under a variety of conditions. Determination of viscosity using the Marsh funnel.

Determination of viscosity and/or gel strength using a direct-indicating viscometer.

The viscosity of drilling fluid is a function of:

- Viscosity of the continuous phase or the base liquid;
- The size, shape and solids particles in the mud which is represent it by the plastic viscosity;
- The inter-particle force represents it by the yield point.

The plastic viscosity is the resistance to flow caused by the friction between solid particles. The yield point is the resistance to the initial flow or the stress required to start flowing. The yield point is measured under flowing conditions.

Reducing viscosity in any drilling fluid can be achieved by:

- Reduction of solids by mechanical treatment or dilution;
- Neutralization of attractive forces between particles [3; 4].

**Mud weight or density**

The density is the weight per unit of volume. During operations mud weight has to be well controlled and need adjustment. If the mud weight is less than the required level of density to drilling safely can permit the formation fluids to flow into the well and lead to well control situation and if it is higher than the appropriate level it can lead to lost circulation situations. Mud weight were tested by 4-scale Metal Mud balance. The real mud weight under circulation is greater than the density while drilling fluid is in static. This density is called equivalent circulating density (ECD). When designing hydraulics, the ECD has to be less than fracture gradient [5].

**Filter cake**

The filter cake is formed when mud solids deposit on the walls of the hole. The filtration is the loss of fluids from mud into the formation. The main objective of controlling fluid loss is forming thin filter cakes while drilling through permeable formations and preventing excessive fluid loss (filtrate).

Loss of drilling fluids in formation can lead to high water consumption and thick filter cake which can cause a tight hole, increased torque and consequently lead to stuck pipe.

**Solids content**

Solids can be:

- Added to the drilling fluid in order to increase viscosity or weight;
- Accumulated in the fluid like drilled cuttings or disintegrated clay particles.

The treatment of solids has to be effective to remove undesired solids which do not contribute to beneficial properties.

**Gel strength**

Gel strength represents the attractive forces under static conditions (non-flow conditions). Contrary to gel strength, the yield point represents the attractive forces under flowing conditions. The gel strength gives an indication of the required pressure to initiate flow after ceasing circulation for period of time. Also, it gives an indication about the ability of the drilling fluid to suspend cuttings when mud is stationary.

Gels are classified into two types:

- Progressive that starts low but increase with time;
- Fragile that starts high and increase slightly with time.

**Toxicity**

The environmental and toxicity standards of the region in which the fluid is being used will require testing either of the whole drilling fluid or of its individual components. Toxicity tests generally are used for offshore applications. An approved laboratory can perform the proper testing to ensure compliance of the fluid or its components.

**Fluid rheology**

Fluid rheology is an important parameter of drilling-fluid performance. For critical offshore applications with extreme temperature and pressure requirements, the viscosity profile of the fluid often is measured with a controlled-temperature and -pressure viscometer (e.g., the Fann iX77 Rheometer). Fluids can be tested at temperatures of < 35 °F to 500 °F, with pressures of up to 20.000 psia.

Cold-fluid rheology is important because of the low temperatures that the fluid is exposed to in deepwater risers. High temperatures can be encountered in deep wells or in geothermally heated wells. The fluid can be under tremendous pressure downhole, and its viscosity profile can change accordingly.

**Fluid loss**

If fluid (or filtration) loss is excessive, the following can occur:

– Formation instability;
– Formation damage;
– Fractured formation and loss of drilling fluid.

In the field, LP/LT(Low Pressure/Low Temperature) and HP/HT(High Pressure/High Temperature) fluid-loss tests are performed routinely. Fluid loss also can be measured under dynamic conditions using the Fann Model 90 Dynamic Filtration System, which incorporates a rotating bob to provide fluid shear in the center of a ceramic-filter core. The fluid is heated and pressurized. Fluid loss is measured radially through the entire core, giving a sophisticated simulation of the drilling fluid circulating in the wellbore.

**Particle plugging**

The particle-plugging test (PPT) often is used to evaluate the ability of plugging particles added to a fluid to mitigate formation damage by stopping or slowing filtrate invasion into a core. A PPT uses an inverted HP/HT-filter-press cell that has been fitted with a ceramic disk as a filtering medium and is pressurized with a hydraulic cylinder. Ceramic disks with different mean pore-throat diameters are used to simulate a wellbore wall. A PPT typically is run with a 2.000-psi or higher differential pressure. The spurt loss and total fluid loss are measured over a 30-minute period. The cell is inverted, and fluid loss is measured from the top of the cell to eliminate the effects of fluid settling.

**High-temperature fluid aging**

Over time, high temperatures can degrade the components of a drilling fluid, and alter its performance. High-temperature aging of the fluid is conducted to assess the impact that temperatures > 250 °F have on performance. Fluid can be aged statically and dynamically. In the static-aging process, the fluid is placed in a pressurized cell, and allowed to stand without rolling at the desired test temperature for a desired length of time (rarely < 16 hours). This simulates the stress the fluid might be subjected to during static periods in the wellbore (e.g., logging and tripping). In dynamic aging, the fluid is rolled in a pressurized cell at the desired test temperature to simulate the fluid under drilling conditions. After undergoing aging, the fluid can be evaluated using the same tests that are applied to non-aged fluid.

**Shale stability**

Reactive shales cause many difficulties in a drilling operation. Fluids should be designed to mitigate these shale problems. Along with erosion testing, four other distinct tests are used to assess the interaction between the drilling fluid and shale: capillary suction time (CST), return permeability, X-ray diffraction and particle-size distribution (PSD).

**CST**

The CST test investigates the chemical effects of the drilling fluid on the dispersive properties of shale and active clays. The CST test measures filter-cake permeability by timing the capillary action of filtrate onto a paper medium. Changes in permeability then can be related to the inhibitive characteristics of the fluid [4].

**Return permeability**

When drilling reaches a hydrocarbon-bearing zone, of great concern is the potential to damage the formation and thereby to reduce the ability of the well to produce hydrocarbons. A return-permeability test can reveal formation damage, and can be conducted using a return permeameter.

**X-ray diffraction**

Knowing the mineral composition of a formation to be drilled is important for determining how the drilling fluid will react with the formation, and how to prevent potential drilling problems. Fluid labs use X-ray diffraction to determine the mineralogical composition of shale or cuttings. They expose a

crystalline mineral sample to X-ray radiation, and compare the resultant diffraction pattern to known standards to determine which minerals are present in the sample.

**Result and discussions**

Not only our investigations but also the American Petroleum Institute (API) publishes documents relating to oilfield standards, including drilling fluids testing procedures. As with any laboratory procedure requiring the use of potentially hazardous chemicals and equipment, the user is expected to have received proper training and knowledge in the use and disposal of these potentially hazardous materials. The user is responsible for compliance with all applicable local, regional, and national requirements for worker and local health, safety, and environmental liability.

Ivestigations of physical chemical properties of drilling fluids are given on Figire 1.

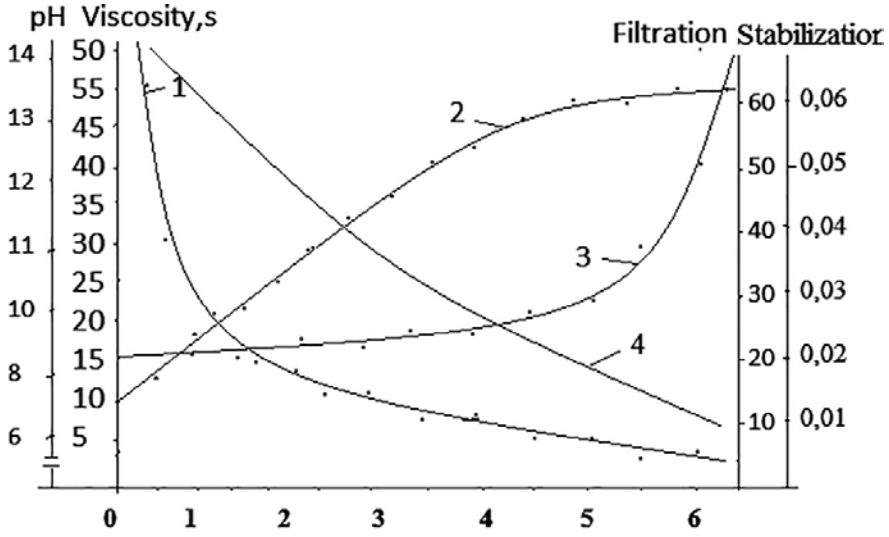


Concentration of reagent MBR,%

Figure 1. Dependence of water filtration (1), pH(2), Viscosity (3) and stabilization index (4) from concentration of CCR

The results of ıınvestigations show that on basis of the chemical reagent MBR, CMC and barite we can receive weighted drilling fluid with a density of 1.55–2.40 g/cm$^3$. The pH of the heavy mud on basis of the composite chemical reagent reaches 9–10 or without the addition of caustic soda. Concentration barite is 40–60%. The composite chemical reagent also has a positive effect on the flow properties as well as filtering solution decreased from 12 to 5 cm$^3$/30 min. Stabilization drilling fluid is one of the main physic-chemical property of drilling mud. Stability drilling fluid is ability of solution to hold particle weighted distribution. It determinates quantity difference of density bottom and top half of the drilling fluid sediment in 24 hours.

Table 1.– Typical Field Tests For WBF

| | |
|---|---|
| Drilling-fluid density | Mud weight, in ppg or equivalent unit of measure, as appropriate to the region [e.g., specific gravity (SG)]. |
| Viscosity | Viscosity exhibited when a specific quantity of fluid is poured through a Marsh funnel (typically recorded in seconds per quart). |
| Rheology | Rheological properties exhibited at various rotational speeds using a viscometer (also called rheometer). The Fann* 35 viscometer can test the fluid at multiple speeds and temperatures to give a detailed viscosity profile for the fluid. |
| Gel strength | Suspension characteristics developed over specified time intervals. |

| | |
|---|---|
| Filtration | Surface indication of filtrate invasion into the near wellbore (also called fluid loss). Performed under LP/LT conditions and HP/HT conditions as required. |
| Retort analysis | Percentages of water, oil, and solids making up the active system. |
| Sand content | Percentage of sand in the active system. |
| Methylene blue capacity | Clay content in the active system [also commonly called methylene blue test (MBT)]. |
| pH | Indication of system acidity or alkalinity. |
| Chemical analysis:<br>Alkalinity/lime content<br>Chlorides<br>Total hardness (calcium) | Indication of variations from base-fluid formulation caused by surface treatment and/or influx or contamination from downhole formations. |

[*] *Fann is the registered name for fluids-testing equipment provided by Fann Instrument Co., Houston*

Extensive testing of the fluid is performed in the design phase of the fluid, either to achieve desired fluid characteristics or to determine the performance limitations of the fluid.

Laboratory testing aids in fluid design and expands the capacity to monitor and evaluate fluids when field-testing procedures prove inadequate. Some laboratory tests are identical to field-testing methods, whereas others are unique to the laboratory environment. In the laboratory setting, testing and equipment should determine following properties for drilling oil and gas wells:

- Toxicity;
- Fluid rheology;
- Fluid loss;
- Particle plugging;
- High-angle sag;
- Dynamic high-angle sag;
- High-temperature fluid aging;
- Cuttings erosion;
- Shale stability;
- Capillary suction;
- Lubricity;
- Return permeability;
- X-ray diffraction;
- Particle-size distribution (PSD).

Investigations show the successful oil well drilling depends largely on a good mud Program. During drilling, mud provides sufficient hydrostatic pressure, removes drill cuttings and cools drill bits. Mud additives are always required to provide sufficient hydrostatic pressure to ensure borehole stability. Barium Sulphate ($BaSO_4$) also known as barite is the prevalent weighting material but there is need to develop local materials to augment the use of Barite. This study was aimed at assessing the suitability of galena, a lead sulfide (PbS), as an alternative weighting material in drilling fluids.

**Conclusions**

Based on the above results, we can conclude that the density, stability, viscosity and filtration of drilling fluids play main role to drill oil and gas wells without accident. Investigations show that safety drilling oil and gas wells depend on geological conditions and the optimum apparent viscosity value is approximately 40–60 s, for filtration value is 3–8 $sm^3$/30 min, for density value according to the layer pressure and for pH value is 9–10 for water based drilling fluids.

## References:

1. API RP 13-$B_1$. Recommend Practice for Field Testing Water-Based Drilling Fluids, third edition. 2003. Washington, DC: API.
2. API RP 13-$B_2$. Recommended Practice Standard Procedure for Field Testing Oil-Based Drilling Fluids, third edition. 1998. Washington, DC: API.

3. Patel A. et al. Designing for the Future–A Review of the Design, Development and Testing of a Novel, Inhibitive Water-Based Mud. 2002. Paper presented at the AADE Annual Technology Conference Drilling and Completion Fluids and Waste Management, Houston, 2–3 April. AADE-02-DFWM-HO-33.
4. Kobilov N. S., Negmatova K. S., Sharifov G. N., Rakhimov X. Y. Composite chemical reagent for stabilization heavy mud for drilling salt-anhydrite layer of oil and gas wells // European applied science. II. Germany, 2016.– P. 50–52.
5. Negmatova K. S., Negmatov S. S., Salimsakov Yu. A., Rakhimov H. Y., Negmatov J. N., Isakov S. S., Kobilov N. S. Structure And Properties of Viscous Gossypol Resin Powder. AIP Conference Proceedings 1459, USA, – 300. 2012.– P. 300–302.
6. Https://Doi.Org/10.1063/1.4738476.
7. Komila Negmatova, Shodilbek Isakov, Nodir Kobilov, 2012. Effective Composite Chemical Reagents Based on Organic And Inorganic Ingredients For Drilling Fluids Used In The Process Of Drilling Oil Wells // Advanced Materials Research. Trans Tech Publication, Switzerland.– Vol. 413.– P. 544–547.
8. Kobilov N. S., Dusmurodov E. B., Kodirov S. A., Khidirov M. Q., Khujamov A. Research and development of effective composite chemical reagents for drilling fluids. An International Multidisciplinary Research Journal. ISSN: 2249–7137.– Vol. 10.– Issue 10. 2020. URL: https://saarj.com
9. Kobilov N. S., Kamolova Z., Shukurov A., Xushnazarov Sh., Sulaymonov I., Khalimov A., Abdurakhmonova N. Development of New Composite Chemical Reagents and Their Implementation/ International Journal of Advanced Research in Science, Engineering and Technology, – Vol. 8.– Issue 1.– January 2021.– P. 16453–16457. URL: https://ijarset.com
10. Kobilov N. S., Negmatov S. S., Yu. Salimsakov A., Sobirov B. B., Negmatova K. S., Rakhmanov B. Sh. Research and Development of Manufacture Technology of Polymeric Composite Materials of Electrotechnical Purpose Filled with Hydrolytic Lignin. 2008. AIP Conference Proceedings.– Vol. 1042.– Issue 10.1063/1.2989016/ URL: https://doi.org/10.1063/1.2989016

**https://doi.org/10.29013/AJT-23-5.6-20-24**

*Savitskiy Andrey Georgievich,*
*PhD, Senior Researcher,*
*Salokhiddinov Abdulkhakim Temirkhudjaevich,*
*D. Sc. in Engineering, Professor,*
*Radkevich Maria Viktorovna,*
*D. Sc. in Engineering, Professor,*
*Shipilova Kamila Bakhtiyarovna,*
*PhD, Senior Lecturer, National Research University*
*"Tashkent Institute of Irrigation and Agricultural Mechanization Engineers",*
*Republic of Uzbekistan, Tashkent*

# REVIEW OF MATHEMATICAL MODELS FOR THE REPRESENTATION OF A CONTINUOUS, TWO-COMPONENT, TWO-PHASE MEDIUM

**Abstract.** The paper analyzes various approaches to modeling the motion of a continuous two-component two-phase medium, reviewing the history of development and the problems of calculation and prediction of aerodynamic and hydrodynamic phenomena. It is revealed that the existing models cannot be used for small-scale phenomena. A search for finite-difference approximations to dynamic models is needed for such phenomena.

**Keywords:** general circulation, scale, instability, hydrostatics, Navier-Stokes equations.

**Introduction.** Modelling of solid, two-component, two-phase medium is of interest in the study of circulation processes in water and air, for pollution dispersion analysis, etc. At present, there are a number of different approaches to modeling, many mathematical models have been created, but the development of this direction continues.

The aim of this article is to analyse existing directions of mathematical modelling of continuous, two-component, two-phase environment and to evaluate possibilities of using existing models for calculation of local climatic comfort zones (microclimate systems).

**1. Classification of mathematical models of air mass movement**

The hierarchy of mathematical models according to their degree of detail can be represented as follows:

Atmospheric general circulation models with computational cell size of 10–100km.

Regional atmospheric models with a grid cell size of 1–10 km.

Atmosphere models with vortex calculations cell size 10–100m.

Turbulence models in the gas medium, computational cell size 1–10 mm.

A separate consideration should be given to integrated ocean-atmosphere models of general circulation models, which are much more complex and comprehensive.

At present, there are no computer facilities capable of calculating all listed model types in such a way as to evaluate both turbulent phenomena and general atmospheric circulation. Accounting for the interaction between the atmosphere and ocean complicates the entire computational process considerably. This is due to the huge difference in velocities of water and air masses. The time step limitations generate such a significant schematic (computational) viscos-

ity that it becomes the dominant factor, masking the adequate reality of water and air masses movements.

2. Historical analysis of the development of mathematical models of air and water mass movement.

Let's take a closer look at the history of the development and emergence of computational aerodynamics.

The basis of theoretical and computational aerohydrodynamics are Navier-Stokes equations. The process of constructing systems of equations describing the motion of coupled media and named Navier-Stokes equations was completed at the beginning of the 19th century (about 1810–1820).

For more than 100 years, many scientists made many efforts to solve the derived equations of hydrodynamics. The hydrodynamic equations were so complex that there was not even an attempt to solve them in their entirety. Only the simplest problems, such as the flow of a cylindrical and spherical body by a laminar incoming flow, could be solved [7].

At the beginning of 1900, the development of similarity theory began. It was the time when physical analogues of processes and phenomena under study were reduced in size. Large replicas of reservoirs, large numbers of wind tunnels and the like were built. The similarity theory clearly stated that it was impossible in principle to build a reduced physical copy of the phenomenon under study in such a way that a complete correspondence between the phenomenon and its reduced model could be achieved. It is impossible to provide equal scaling of the Reynolds, Mach, Struhal, etc. parameters at the same time. The difference between the behaviour of a fluid or gas in models and reality is particularly strong when there is a significant difference in the size of the phenomenon and the model of the phenomenon. Huge wind tunnels and huge models of dams and river sections were built. The physical model of a section of the Amu Darya River at the new SANIIRI site was up to 15 metres wide and over 100 metres long. Even such huge physical models could not meet the demands of construction and design.

In 1956, Rakhmatullin published a system of equations of motion for multiphase media [12]. This event became an impetus for the emergence of a whole group of scientific schools of multiphase flow motion theory.

Especially rapidly, the multiphase flow motion theory began to develop in the Uzbek SSR. The School of Computational Aerodynamics of F. B. Abutaliev, Corresponding Member of the Academy of Sciences of the Uzbek SSR, studied only the atmospheric phenomena and climatic phenomena prediction using numerical methods.

The second school under the leadership of T. D. Dzhuraev conducted academic research of multiphase flow equation systems, their stability and uniqueness of solutions. Particular attention was paid to problems with unknown boundary of solution domain. That is, those hydrodynamic problems in which the position of the free surface limiting the fluid flow depends on the motion of the fluid itself were solved.

Also the hydrodynamics was considerably developed at the Central Asian Hydrometeorological Institute (CAHMI), which was one of the first recipients of high-performance computers of the IBM-22 and IBM-32 generation. This made it possible to build mathematical models of the atmosphere and to solve complex systems of equations. The first significant works on the construction of mathematical models of the atmosphere began to appear from 1970. One of the first significant works was published at the CAHMI in 1978 [5]. This work is interesting only in the depth of theoretical material and in writing the equations of motion for multiphase media in the most general, but also sufficiently complete form.

At that time outside the USSR there was no progress in creating mathematical models of atmospheric circulation. Computational fluid mechanics in Europe and the USA concentrated mainly on highly specialized problems related to the flow around bodies with complex configurations using the finite element method. The main customer of such

research was the military-technical complex, so very often one could find in the literature descriptions of mathematical models adapted to calculate the aerodynamics of fast-moving objects – aircraft, machines and ships [1; 2].

Interestingly, this time coincides with the degradation of analogue modelling – the study of hydrodynamic phenomena on scaled-down physical models. By 1990, analogue modelling had disappeared as a class of research in its own right.

Computational fluid mechanics around the world are trying to solve the Navier-Stokes equations with finite difference methods. The finite difference method makes it easy to switch the generated solution algorithm for one problem to another problem. However, when solving full (or sufficiently full) Navier-Stokes equations and applying explicit schemes, the so-called "dynamic instability" occurs. All the characteristics of the solution begin to change sinusoidally, but the amplitude of these harmonic oscillations increases exponentially. The calculation terminates with an emergency stoppage of the computational process and nothing has been done to deal with this type of instability. Attempts to introduce artificial viscosity into the calculation to stabilize the dynamical instability failed. Tridiagonal matrices of algebraic equations were formed only for one-dimensional problems solved by Navier-Stokes equations, which is of little interest.

At that time in Novosibirsk branch of the USSR Academy of Sciences G. I. Marchuk finds and substantiates the method of subordinate and then factor splitting of multidimensional equations of motion of coupled medium (Navier-Stokes equations). Three-dimensional problems are decomposed into a series of sequentially solved one-dimensional problems. First everything related to motion along one axis, then another axis and then a third axis is computed. Each solution is the initial state for finding the next solution. The result is the ability to apply implicit calculation schemes using the economical 'forward and backward run' algorithm.

The solution obtained, of course, has some fluctuation, but it is stable, and this is the main thing. G. I. Marchuk proves the singleness theorem and existence of a solution for subordinately split hydrodynamic problems with a certain small given accuracy. G. I. Marchuk formed the Novosibirsk school of computational hydrodynamics, which published many articles dedicated to the calculation of circulations in the seas and oceans [8].

A number of scientists begin to actively apply the achievements of Novosibirsk hydrodynamicists in aerodynamics. Models of water circulation are created first for separate seas [11], parts of oceans [4], then oceans as a whole, and then global mathematical models of water circulation in the World Ocean appear. At the same time, G. I. Marchuk is engaged in the development of climatic mathematical models and the development of methods for their solution [6; 8; 9].

The development of the Novosibirsk scientific school coincided with the development of run-time methods for solving algebraic linear equations of a special kind. It turned out that for the case when algebraic equations can be written in the form of tridiagonal matrix with predominance of terms located on main diagonal, then they are solved by simple algorithm called "forward and backward run" [3, 13].

One of the most important conditions for solvability of the Navier-Stokes equations to describe the circulation in the seas and oceans was the so-called "truncation" of the vertical component of the equation of motion to the hydrostatic state. As a result of this action it was possible to create easily a calculation algorithm calculating the vertical component of velocity through the continuity equation for an incompressible fluid.

However, in this case it is impossible to take into account the hydrodynamic pressure and its influence on the motion of a cohesive medium. It was considered that the motion of a cohesive medium provides only hydrostatic pressure. However, the main achievement of this calculation was that the incompressibility of the fluid no longer created the danger of sound waves moving at infinite velocities.

**3. Current problems in solving aerohydrodynamics problems**

More than 40 years have passed but the practical approach to solving aerohydrodynamics problems has remained practically unchanged [10]. Most of the problems on circulation of water and atmospheric masses were solved by the method of establishment, which was theoretically developed in Novosibirsk by a group of scientists headed by G. I. Marchuk. But during the method of establishment it was thought without proof that even under changing boundary conditions the system is always in a stable equilibrium state. At the same time, inertia in the processes of mixing water and atmosphere was never calculated, most likely because any artificial numerical filters were used to exclude wave processes on the free surface of water or the upper bounding layer of the atmosphere. The filters have always been subjective and have in fact determined the ability of the current system to be driven entirely by changing boundary conditions. Calculations took a long time as computers of that time could carry out one calculation cycle in 5 seconds and it was not possible to speed up the process.

It means that the advance of the real process on a coarse grid could be tenfold. This means that calculation of a day would take 2.5 hours.

But even such a calculation necessarily required some heuristic filter to cut off the oscillations, because no one was able to reach the maximum allowable time step. Most characteristic was that the duration of the calculation was almost the same time as the real process.

Nowadays, with the advent of super-fast computers, the situation has improved, but not dramatically. Weather forecasts for at least a week ahead are still not achievable without the introduction of some artificial heuristic oscillation filters.

Parallel to the development of computational methods for solving the equations of aero-hydrodynamics, in-depth research on the development of the theory of interpenetrating motion of multiphase media continues. The equations of multiphase media were first written in phase space. This is a four-dimensional space in which there are three spatial coordinates and one additional coordinate – the characteristic dimensions of one of the phases represented by discrete entities of different sizes. For gas-liquid medium such parameter may be different diameters of spherical water droplets. The equations are written in a non-stationary form, specifically in a kinematic form (so-called Boltzmann equations). This model was developed by A. A. Dzhuraev and Y. M. Denisov [5], who completely uncovered the mechanism of motion of water mass between discrete droplets and the surrounding air mixture of dry air and water vapor.

By the end of 2021, there were more than a dozen atmospheric mathematical models being used for short-term weather forecasting – no more than 10 days ahead – and not everywhere is possible. The best mathematical models are used in Israel (7–10 days lead time) and relatively good ones are used in Japan and USA.

The website https://hmong.ru/wiki/Climate_model provides a list of mathematical models currently in active use to study atmospheric circulation.

All these models contain general achievements of Novosibirsk scientists of G. I. Marchuk school and in case of application of implicit calculation schemes – achievements of A. A. Samarsky: "cutting down" of vertical equation of motion to hydrostatic equation, incompressibility of continuous medium (including air in climate models) and possible application of economical solution of algebraic equation systems which can be written in form of tridiagonal matrix (application of implicit finite-difference schemes).

**Conclusion.** None of the models considered can be used as a basis for the investigation of microcirculation of water droplet-gas systems in microclimate control areas for the following reasons:

1. The scale of the phenomena is incommensurable.

2. The scales of existing models are hundreds of kilometres, and for scales of tens of metres "downsizing" to hydrostatics is unacceptable.

3. Gas is assumed to be a compressible medium.

4. The computational viscosity of implicit schemes in solving our problem is unacceptable.

Therefore, the objectives of further research are:

– the construction of a complete mathematical model of the dynamics of a multicomponent and multiphase medium;

– investigation of finite-difference approximations to solve the obtained algorithms;

– development of the algorithm for the solution of the stated tasks.

## References:


1. Anderson D., Tannehill J., Pletcher R. Computational fluid mechanics and heat transfer. In 2 vols.– Moscow: Mir, 1990.– 726 p.
2. Batchelor J., Moffat G. Modern hydrodynamics. Advances and problems. Journal of fluid mechanics. Special issue celebrating the 25th anniversary of the journal and containing editorial reflection on the development of fluid mechanics.– Moscow: Mir, 1984.– 504 p.
3. Godunov S. K., Ryabenkiy V. S. Differential Schemes.– Moscow: Nauka, 1977.– 440 p.
4. Demyshev S. G., and Korotayev G. K. Numerical Experiment in Calculating Equatorial Circulation Based on Conservative Model // Marine Hydrophysical Journal,– No. 4. 1989.– P. 13–23.
5. Denisov Yu. M., Dzhuraev A. A. Mathematical model of some microphysical processes in a cloud // Proceedings of SARNIGMI named after V. A. Bugayev (81–162). Mathematical Modelling of Hydrological Processes.– Moscow: Gidrometeoizdat, 1981.– P. 53–59.
6. Kordzadze A. A. Mathematical Problems of Solving Problems of Ocean Dynamics. Novosibirsk. VTSO of Academy of Sciences of USSR, 1982.– 148 p.
7. Landau L. D., Lifshits E. M. Theoretical Physics. Hydrodynamics.– Vol. VI. 3 ed.– Moscow, Nauka, 1986.– 636 p.
8. Marchuk G. I. Mathematical Models of Circulation in the Ocean.– Novosibirsk.– Nauka, 1980.– 288 p.
9. Marchuk G. I., Kurbatkin G. P. Numerical Weather Forecasting of Earth and Universe. – Novosibirsk: Nauka, 1978.– P. 37–43.
10. Mingalev V. S., Mingalev I. V., Orlov K. G. Studies of atmospheric circulation using three-dimensional mathematical models developed at the Polar Geophysical Institute during the last two decades // Bulletin of Kola Scientific Centre RAS, Polar Geophysical Institute.– 4(23). 2015.
11. Pavlushin A. A., Shapiro N. B., Mikhaylova E. N. Influence of basin shape on circulation formation in the Black Sea. Marine Hydrophysical Institute of RAS. Sevastopol. 2016.– 15 p.
12. Rakhmatullin H. A. Fundamentals of gas dynamics of interpenetrating motions of compressible media. Applied mathematics and mechanics.– 1956.– T. 20, Issue. 27.– C. 184–195.
13. Samarskiy A. A., Gulin A. V. Numerical methods.– Moscow. Nauka, 1989.– 432 c.– ISBN5-02-013996-3.

# Section 4. Physics

**https://doi.org/10.29013/AJT-23-5.6-25-28**

*Utamuratova Sharifa Bekmuratovna,*
*professor, Director of the Institute of Semiconductor Physics and Microelectronics at the National University of Uzbekistan,*
*Tashkent, Uzbekistan*

*Rasulov Voxob Rustamovich,*
*associate professor of Fergana State University*
*Fergana, Uzbekistan*

*Isomiddinova Umida Mamurjonova,*
*teacher of the Kokand State Pedagogical Institute*
*Fergana, Uzbekistan*

*Kodirov Nurllo Ubaidullo ogli,*
*doctoral student of Fergana State University*
*Fergana, Uzbekistan*

## INTRABAND MECHANISM OF THREE-PHOTON ABSORPTION OF POLARIZED RADIATION IN DIAMOND-LIKE SEMICONDUCTORS

**Abstract.** The polarization and frequency-polarization dependences of the linear-circular dichroism and light absorption coefficients in semiconductors of cubic symmetry, caused by vertical three-photon optical transitions between the states of the spin-orbit splitting and conduction bands, are calculated.

**Keywords:** three-photon optical transitions, spin-orbit splitting band, conduction band, linear-circular dichroism, light absorption, semiconductor.

**Introduction.** Currently, the main research in the field of multiphoton absorption of light is carried out in wide-gap semiconductors, since a number of their physicochemical properties have been studied in depth and in more detail. In this respect, multiphoton effects occurring in narrow-gap crystals have been little studied both in theoretical and experimental aspects. The main reason for this is that the theoretical study of a number of photon-kinetic phenomena in narrow-gap crystals requires the use of not only the Luttinger-Kohn approximation, but also the multiband Kane approach. In the latter case, theoretical calculations are performed using matrices of at least $6 \times 6$ or $8 \times 8$.

The first works on two-photon interband transitions in crystals were carried out in the early 1960 y., shortly after the appearance of lasers [1–3]. When calculating the matrix elements of two-photon transitions in crystals, perturbation theories were used in the field of an unpolarized

electromagnetic wave [2; 3], where the two-band Kane model was used.

In [4–10], both theoretically and experimentally, linear-circular dichroism (LCD) of two- and three-photon absorption of light in crystals of cubic symmetry was investigated. However, the question of the polarization and frequency-polarization study of three-photon interband absorption of light in crystals of cubic symmetry, caused between the states of the spin-orbit splitting band and the conduction band in the Kane approximation, remained open.

**Results and discussion**

**Three-photon linear-circular dichroism**

In our previous works, three-photon optical transitions originating from the state of the spin-orbit splitting subband into the conduction bands were analyzed and it was shown that they are 10 different transitions [11], which differ from each other by virtual states. As indicated in [11] (see formula (4)), the multiphoton interband light absorption coefficient has two terms, one of which describes the sum of partial light absorption coefficients, and the second contribution to the multiphoton light absorption coefficient due to the interference terms of the matrix elements of the above optical transitions in crystals of cubic symmetry.

First, we will analyze the polarization dependences of interband optical transitions arising from the state of the spin-orbit splitting subband $|SO,\pm 1/2\rangle$ into $|c,\pm 1/2\rangle$ conduction bands (i.e., three-photon transitions of type $|SO,\pm 1/2\rangle \Rightarrow |c,\pm 1/2\rangle$), where we take into account that for linearly polarized light: $|e'_z|^2 = \cos^2\alpha$, $|e'_\pm|^2 = 1 - |e'_z|^2$, for circularly polarized light $|e'_z|^2 = \frac{1}{2}\sin^2\beta$, $|e'_\pm|^2 = 1 - |e'_z|^2 \mp P_{circ}\cos\beta$, where $\alpha\,(\beta)$ is the angle between the polarization vectors $\vec{e}$ (the wave vector of the photon $\vec{q}$) and the wave vector of current carriers ($\vec{k}$), $e'_x, e'_y, e'_z$ are the projections of the polarization vector of light along the axis $x', y', z'$, associated with the direction of the wave vector of electrons $\vec{k}\,(\vec{k}\|z')$, $e'_\pm = e'_x \pm ie'_y$, $\vec{q}$ – is the wave vector of the photon, 99 is the degree of circular polarization of light, and the sign of "$\pm 1/2$" is describes the spin states of current carriers.

Calculations carried out according to the golden rule of quantum mechanics [12] for InSb show that in three-photon transitions of the type $|SO,\pm 1/2\rangle \Rightarrow |c,\pm 1/2\rangle$, the graph of the polarization dependence of the coefficient of three-photon linear-circular dichroism is described in (Fig. 1) and if two virtual states lie in the subbands of the valence band, and Fig. 1, b, if both virtual states lie in the conduction band, and Fig. 1, c, if the initial virtual states lie in the conduction band, and the next ones, in the valence band (in the approximation quadratic in the wave vector in the effective carrier Hamiltonian, some of the optical transitions are forbidden, and the part is nonzero).

In quantitative calculations, the numerical values of the band parameters were taken from [13]. Note here that in the first case, the polarization dependence of three-photon linear-circular dichroism is almost independent of the frequency of light. This means that linear-circular dichroism does not appear in this case, i.e. interband three-photon absorption of light does not depend on the degree of polarization of the light.

Note here that the energy spectra of current carriers in all bands are taken as parabolic, and when the three branches of the band structure of the semiconductor are nonparabolic, then the quadratic dependence of the energy on the wave vector is approximately restored only near the edges of the Brillouin zones.

That. showed that the polarization dependence of the linear-circular dichroism of three-photon absorption of light on the type of optical transitions. Since the matrix elements of some optical transitions have in the numerator the difference in the energies of current carriers, which in a certain region of the frequency of light tends to zero, which leads to an anomalous increase in the spectral dependence of the three-photon absorption coefficient of light, but this phenomenon leads to a noticeable change in the

spectral dependence of linear-circular dichroism, since the coefficient of linear-circular dichroism is defined as the ratio of the probabilities of optical transitions occurring upon absorption of light with linear and circular polarization.

**The three-photon light absorption coefficient**

Let us now analyze the frequency-spectral dependence of the light absorption coefficient for InSb, caused by three-photon transitions of the type. Calculations for the semiconductor InSb show that in three-photon transitions of the type, the graph of the polarization dependence of the coefficient of three-photon linear-circular dichroism is described in Fig. 1, when two virtual states lie in the subbands of the valence band, and (fig. 2), when both virtual states lie in the conduction band (in the approximation quadratic in the wave vector in the effective carrier Hamiltonian, some of the optical transitions are forbidden, and some nonzero).

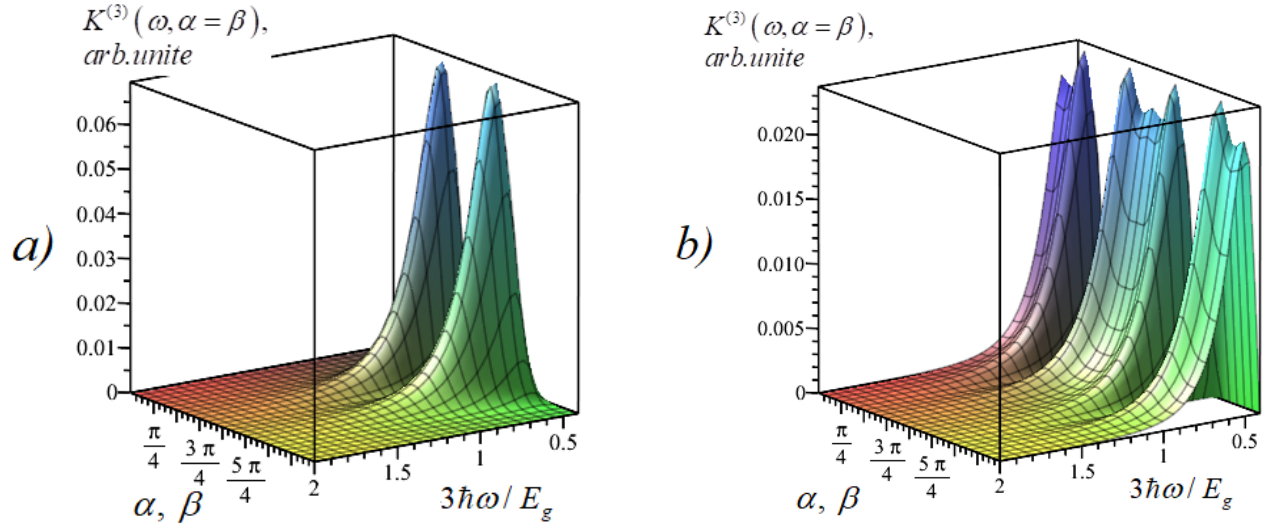


Figure 1. Frequency-polarization dependences of the three-photon light absorption coefficient in GaAs. Curves: a) correspond to circular polarization, curves; b) to linear polarization;

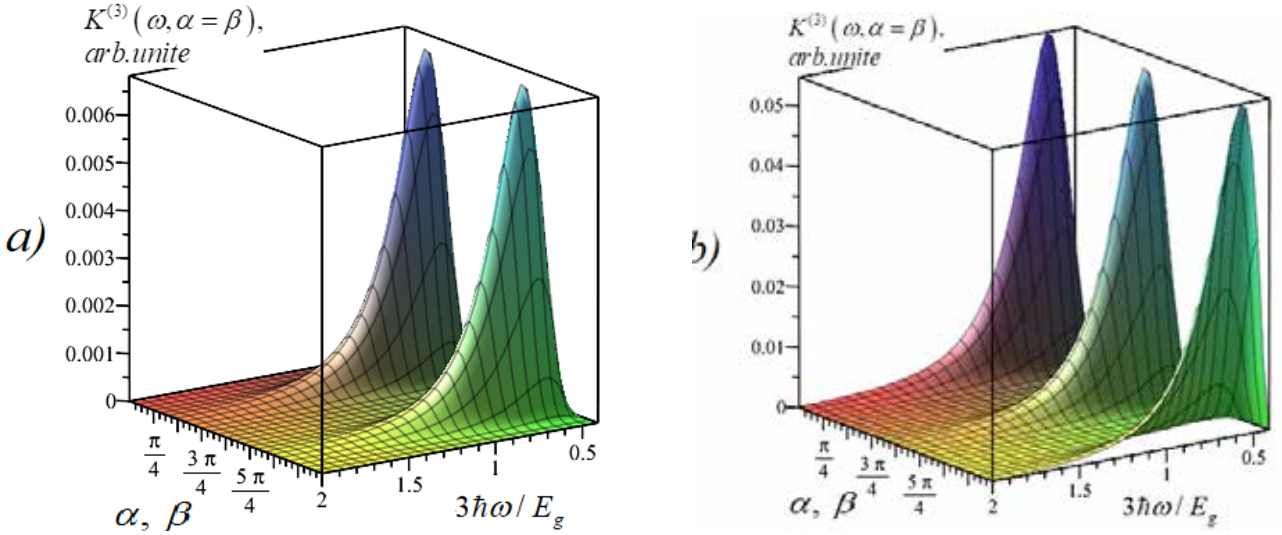


Figure 2. Frequency-polarization dependences of the three-photon light absorption coefficient in GaAs. Curves: a) correspond to circular polarization, curves; b) to linear polarization;

It can be seen from (Figs. 1–2) that the main contribution to the coefficient of three-photon absorption of light is made by optical transitions, in which the initial virtual states lie in the conduction band, and the next ones, in the valence band.

**Conclusion.** From the above results and figures 1–2, it can be seen that both the polarization and frequency-polarization dependences of the linear-circular dichroism and linear-circular dichroism coefficients have several extrema. This is due to the specificity of the Kane model used to study the band structure in narrow-gap crystals. In particular, in the Kane model, some off-diagonal matrix elements of the momentum operator do not depend on the wave vector of current carriers, which does not occur in the Luttinger-Kohn model.

## References:


1. Miller A. A., Johnston J., Dempsey J., Smith C. R., Pidgeon, and Holah G. D. Two-photon absorption in InSb and Hg1-xCdxTe // – J. Phys.– No. 12. 1978.– P. 4839–4849.
2. Comparee C. R., Pidgeeon B. S., Wherrett A. M., Johnston J. Dempsey, and A. Miller: Two-photon absorption in zinc-blende semiconductors // Phys. Rev. Lett.– Vol. 42.1979.– P. 1785–1788 and references therein.
3. Braunstein R. and Ockman N. Optical double-photon absorption in CdS // – Phys. Rev. A. 1964. – Vol. 34.– P. 499–507.
4. Rasulov R. Ya. Polarization optical VA photovoltaic effects in semiconductors with linear and nonlinear absorption of light. Dissertation for thesis. uch. doctor's degree phys.-math. sciences.– St. Petersburg, 1993.– 206 p. (in Russian).
5. Ivchenko E. L. Two-photon absorption and optical orientation of free carriers in cubic crystals // FTT.– T. 14.– Issue 12.– WITH. 1972.– P. 3489–3485. (in Russian).
6. Beregulin E. V., Dvornikov D. P., Ivchenko E. L., Yaroshetskiy I. D. Polarization properties and linear-circular dichroism in nonlinear light absorption in $A_2B_6$ semiconductors // FTT.– T. 9.– No. 5. 1975.– P. 876–886. (in Russian).
7. Arifzhanov S. B., Ivchenko E. L. Multiphoton absorption of light in crystals with a diamond and zinc blende structure // FTT.– Vol. 17. – No. 1. 1975.– P. 81–89. (in Russian).
8. Rasulov R. Ya. Linear circular dichroism in multiphoton interband absorption in semiconductors // FTT.– St.-Petersburg,– T. 35.– Issue 6. 1993.– P. 1674–1678. (in Russian).
9. Rasulov R. Ya. Linear-circular dichroism in multiphoton interband absorption in semiconductors // Solid State Physics.– St. Petersburg,– Vol. 35.– No. 6. 1993.– P. 1674–1677. (in Russian).
10. Rasulov V. R., Rasulov R. Ya., Eshboltaev I. Linearly and circular dichroism in a semiconductor with a complex valence band with allowance for four-photon absorption of light // Physics of the Solid State.– Springer,– Vol. 59.– No. 3. 2017.– P. 463–468.
11. Rasulov V. R., Rasulov R. Ya., Eshboltaev I. M., Qo'chqorov M. X. Interband Multiphoton Absorption of Light in Narrow-Gap Crystals // European Journal of Applied Physics.– Vol. 3.– Issue 5. 2021.
12. Landau L. D., Lifshits E. M. Quantum Mechanics (Nonrelativistic Theory) – Vol. III.– M.: Fizmatlit, 2004.– 800 p. (in Russian).
13. Vurgaftman I. and R. Meyer J., Ram-Mohan L. R. Band parameters for III – V compound semiconductors and their alloys // Journal of Applied Physics.– 89 (11). 2001.– P. 5815–5875. URL: https://doi.org/10.1063/1.1368156.

# Section 5. Chemistry

**https://doi.org/10.29013/AJT-23-5.6-29-35**

*Huseynova Elmira,*
*Shiraliyeva Ulkar,*
*Ismayilova Kamala,*
*Bagirova Ziba,*
*Imanova Nasiba,*
*Rzayeva Aida*
*Azerbaijan State Oil and Industry University Scientific Research Institute "Geo-Technological Problems of Oil, Gas, and Chemistry" Baku, Azerbaijan*

## THEORETICAL ASPECTS INVESTIGATION OF THE STRUCTURE OF PHOSPHORMOLYBDENUM HETEROPOLY ACID CATALYSTS FOR THE OXIDATION OF METHACROLEIN TO METHACRYLIC ACID

**Abstract.** The present study investigates of the structure of phosphormolybdenum heteropoly acid catalysts for the oxidation of methacrolein to methacrylic acid. As a result of the studies of the reaction of oxidative transformation of unsaturated $C_3$-$C_4$- aldehydes into the corresponding acids, the composition of samples with empirical formula was established: $Cs_{0,2-1}\ W_{0,1-1}\ Cu_{0,1-0,5}\ Cr_{0,07-0,4}\ Zn_{2-4}\ P_1\ Mo_{12}\ V_{0,1-0,5}\ (NH_4)_{1-4}\ O_x$

The selected sample for a detailed study of the structure is as follows:

$Cs_{0,7}\ W_{0,2}\ Cu_{0,1}\ Cr_{0,4}\ Zn_3\ P_1\ Mo_{12}\ V_{0,3}\ (NH_4)_{3-4}\ O_{45,5}$ The first sample was prepared from ammonium salts of P, Mo, and V, and the second was based on phosphormolybdenum heteropoly acid. The same evaporation, drying, and calcination conditions were followed in all cases. The calcined aluminum oxide was used as a reference substance. As the results showed, regardless of the catalyst preparation method, increasing temperature up to 430 °C affects its properties. These changes lead to irreversible activity loss and selectivity by 5–6 times. Presented X-ray pictures of samples that have worked for 75 hours in methacrolein oxidation mode indicate that the properties of the catalysts are unchanged. Diffractometers show that the catalyst samples are not amorphous but crystalline. The paper gives IR spectra of the catalyst samples before and after they reached stable activity. Data for the catalysts modified with cesium compared with the original heteropoly acid are presented. It is indicated that the position and relative intensity of several characteristic reflexes on the X-ray diffraction pattern change. The low catalytic activity of the samples revealed is caused by the presence on the surface of ammonia formed during the synthesis of the catalyst heating removes ammonia. The catalyst activity increases more than threefold,

and the selectivity does not change. Heating of freshly prepared catalyst removes crystallization water (~170 °C). A series of experiments were conducted to determine the catalyst's thermal stability limit. Increasing of temperature to 430 °C does not affect its properties. It should be noted that the catalyst decomposition temperature is higher than that of phosphormolybdenum acid (370 °C, 50° higher). This is achieved by modifying it with various additives. Thanks to the conducted research, it is possible to change the catalyst structures to improve their properties.

**Keywords:** phosphormolybdenum, methacrylic acid, methacrolein, molybdenyl, catalysts, conversion, ammonium phosphate, vanadate.

Acrylic and methacrylic acid are industrially produced via the partial oxidation of their corresponding aldehydes, namely acrolein and methacrolein [1–8]. Different catalysts are used for these tasks: mixed-oxides based on Mo, V and W for the acrolein oxidation, and heteropolyacids based on Mo, V and P for the methacrolein oxidation, since the respective other catalyst has a poor performance. To generate a deeper knowledge of the catalytic mechanism, especially of the different properties of the catalysts, the of phosphormolybdenum heteropoly acid catalysts for the oxidation of methacrolein to methacrylic acid [11–20].

The results of tests of a series of modified phosphormolybdenum heteropoly acid catalysts in the reaction of oxidative conversion of unsaturated $C_3$-$C_4$-aldehydes into corresponding acids allowed establishing the optimal qualitative and quantitative composition of samples that meet the empirical formula:

$$Cs_{0,2-7}\ W_{0,1-1}\ Cu_{0,1-0,5}\ Cr_{0,67-0,4}\ Zn_{2-4}\ P_1\ Mo_{12}\ V_{0,1-0,5}\ (NH_4)_{1-4}\ O_x$$

For the study of the structure, selected samples of the composition:

$$Cs_{0,7}\ W_{0,7}\ Cu_{0,1}\ Cr_{0,4}\ Zn_3\ P_1\ Mo_{12}\ V_{0,3}\ (NH_4)_{3-4}\ O_{45,5}$$

prepared in various ways.

Sample № 1 was prepared from ammonium salts of P, Mo, and V by precipitation from an aqueous solution. Ammonium paramolybdate, ammonium phosphate and vanadate, nitrates of Zn, Cs, and other metals included in the catalyst were used. The resulting suspension was dried and calcined.

Sample № 2 was synthesized from phosphorus molybdenum heteropoly acid (water solution $H_3PMo_{12}O_{40} \cdot 26H_2O$), of ammonium carbonate, and nitrates of alkali and other metals; vanadium ions were introduced by dissolving metallic vanadium in the heteropoly acid. This was followed by drying and calcination.

In all cases, evaporation and drying of the suspension were performed at t=125 °C. The following burning regime was observed: 200 °C – 4 h, 260 °C – 2 h, 310 °C – 1 h, 330 °C – 1 h. X-ray studies of the phase composition of the samples were performed by the Debye-Scherrer method on the diffractometer DRON-3 with filtered Cu-K-radiation.

IR spectra were recorded on a spectrophotometer UR-20 at room temperature.

Thermograms of freshly prepared and run catalysts were taken on the derivatograph of Hungarian firm MOM-500. The calcined aluminum oxide was used as a reference substance. The samples were taken in the temperature interval of 20–1000 °C at the speed of 2.5; 5, and 10 °C per minute. The temperature curves (DTA), sample mass (TG), and mass change rate (DTG) were recorded on the thermograms.

Figure 1 shows radiographs of samples freshly prepared and run for 75 h in the methacrolein oxidation mode. The structure of the catalysts remains unchanged during long-term operation. X-ray patterns of the samples correspond to tabulated data for the ammonium salt of 12-molybdenum phosphoric acid [1] with the main values of interplanar distances (d) equal to 8.40; 5.93; 4.16; 3.72; 3.40; 2.93; 2.5; 2.3; 2.07; 1.65. Diffractograms show that the catalyst samples are not amorphous but crystalline. The diffraction peaks belong to the same basic phase of composition: $(NH_4)_3PO{\cdot}12\ MoO_3{\cdot}3H_2O$. The values of interplanar distances and intensities are taken from the reference book [9–11].

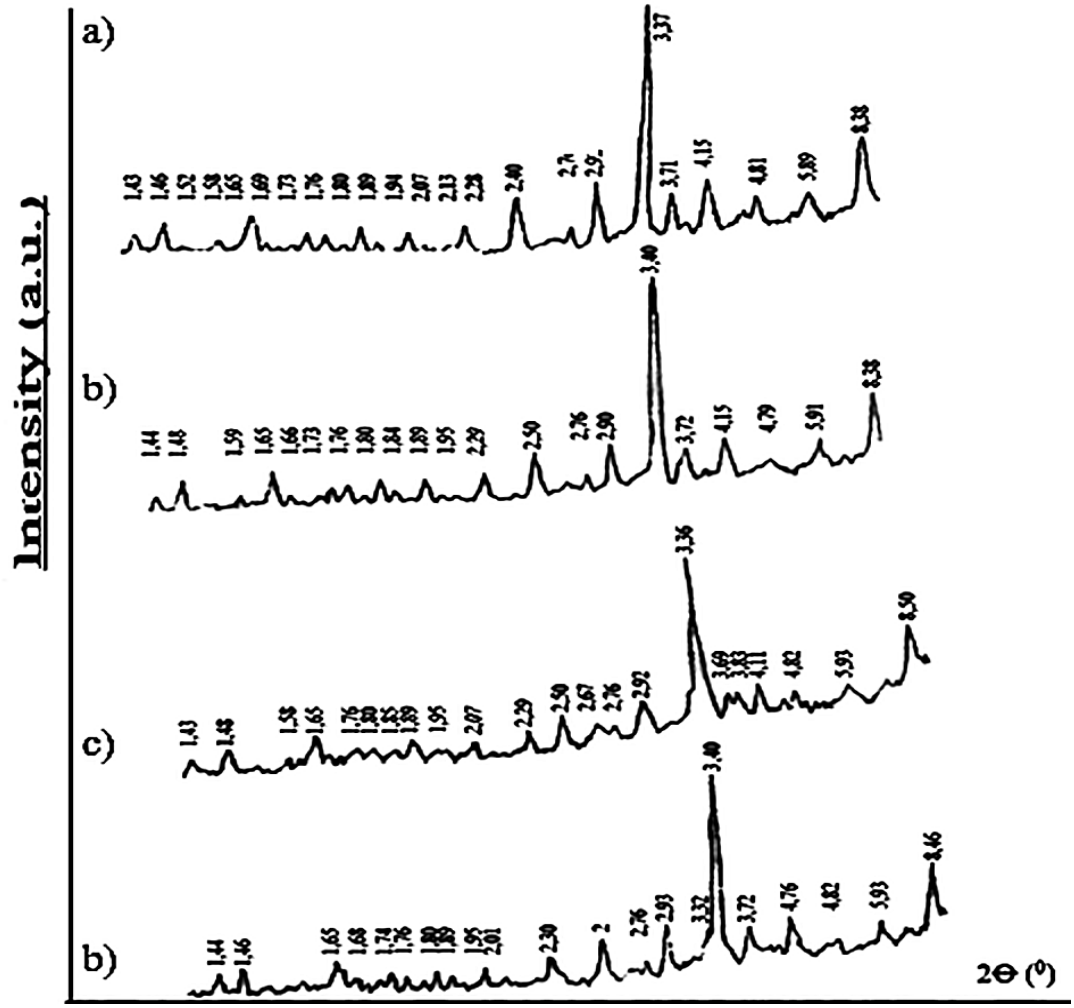


Figure 1. X-ray diffraction patterns of catalyst samples:
a, c) freshly prepared; b, d) worked for 75 hours

According to XRD data, for catalysts modified with cesium, in comparison with the original GDC, the position and relative intensity of several characteristic reflexes on the X-ray diffraction patterns change. Practically, intensive lines corresponding to interplanar distances of 9.90; 4.36, and 1.97 Å in GDC disappear, new ones appear – 8.41 and 2.93 Å, maxima of the most intensive band are shifted from 3.21 to 3.40 Å.

Fig. 2 shows infrared spectra of catalyst samples before and after they reached stable activity. As is known [3; 4], for the initial HPA.The leading absorption bands with maxima at 1065, 965, 870 (w), and 790 (w) cm characterize vibrations of P-O-Mo, Mo = = O, and Mo-O-Mo bonds typical for heteropolyanion $[PMo_{12}O_{40}]^{-3}$. In addition to the usual main absorption bands describing the Keggin cell, there are bands at 1420 $cm^{-1}$ related to ammonium ions in the spectra.

When cesium ions are introduced into the catalyst, the maximum absorption band of the molybdenum group (Mo = O) shifts to 970 $cm^{-1}$ (the M = = O bond increases, and coordination octahedron symmetry changes); the position of the optimal bands remains unchanged. In addition to the 960, 870, 990, and 1060 $cm^{-1}$ absorption bands, 1420 $cm^{-1}$ absorption bands characteristic of $NH_4^+$ ions comprising the heteropoly acid salt or $NH_3$ molecules chemisorbed on the brandsted acid centers or coordinately bound to the catalyst surface are observed. However, the intensity of these absorption bands after a 35-hour

"development" of the catalyst becomes somewhat lower than in the freshly prepared sample. The firmly bound ammonia on the catalytic surface formed during catalyst synthesis and adsorbed on its Brandsted and Luis acid centers causes the low catalytic activity of freshly prepared samples. Additional heating of the catalyst in the reaction mixture removes ammonia. In this case, the activity of the catalyst increases more than threefold, and the selectivity remains constant throughout the activation process and further operation. Experiments on ammonia poisoning of the catalyst synthesized from phosphormolybdenum HPA showed that adsorption of $NH_3$ in 1% of the surface filling leads to its complete deactivation.

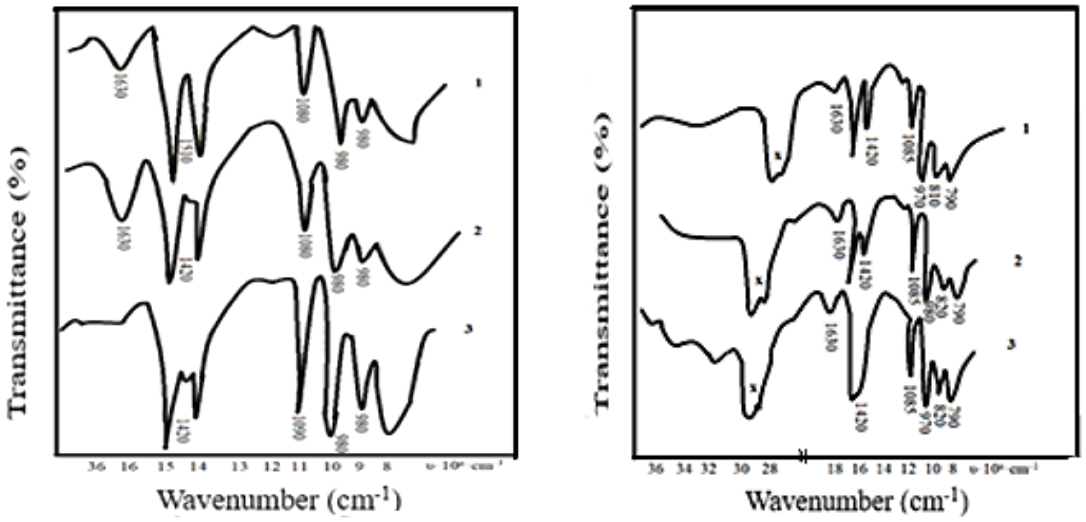


Figure 2. IR spectra of catalyst samples: 1 – Freshly prepared; 2 – Worked for 75 hours; 3 – Working for 170 hours; * – absorption bands of vaseline oil

Thermographic studies were performed for fresh samples, as well as samples that had been in operation for 75 and 175 hours. Due to the similarity of results, derivatograms of only samples of catalyst from phosphorus molybdenum HPA are shown in (fig. 3).

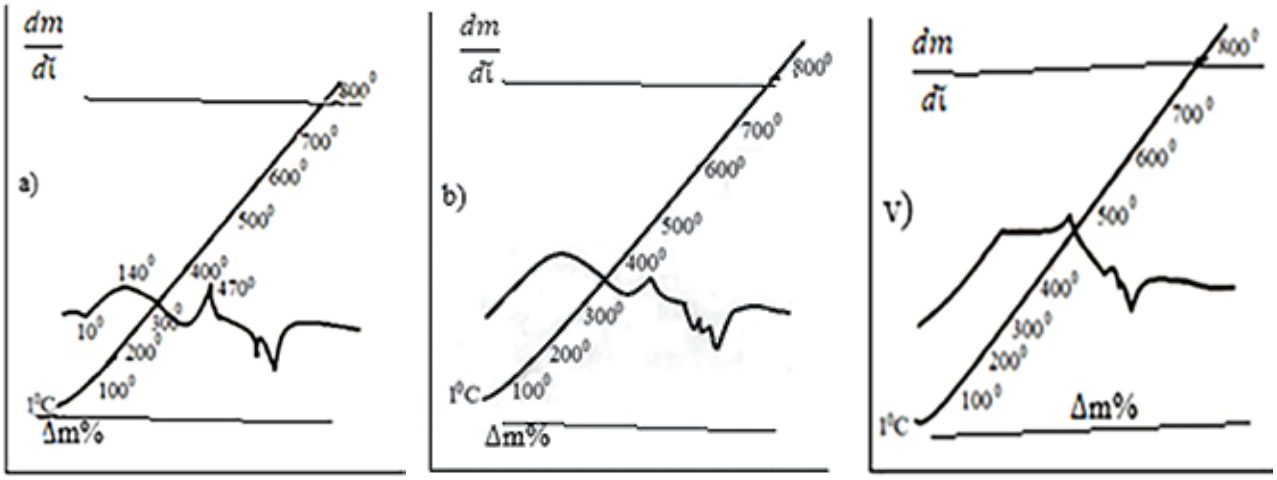


Figure 3. Derivatograms of catalyst sample; a)freshly prepared; b) worked for 75 hours; v) worked for 170 hours

When the freshly prepared catalyst is heated to 200°C, the removal of crystallization water occurs, as evidenced by the endothermic effect in the region of 100–200°C (170°C). The decomposition of the

catalyst begins at t > 430 ˚C, and an exo-effect is observed at 479 ˚C, which corresponds to a clear step of weight loss on the TG curve. This is followed by a series of endo-effects at 560 ˚C and 600 ˚C, which presumably can be attributed to phase transitions of the melting type. At this temperature segment of the TG-curve, there is no mass loss.

In the derivatogram of the catalyst that worked for 75 h, the endo-effect of moisture loss at 170 ˚C is absent. The intensity of the exoeffect decreased at 470 ˚C. A series of subsequent endo-effects repeated with the same intensity, but the endo-effect at 560 ˚C shifted to 580 ˚C.

The sample that had been in operation for a longer time (170 h) was characterized by the disappearance of the exoeffect at 470 ˚C on the derivatogram with a corresponding step loss on the TG curve. The series of endo-effects related to melting is repeated at the same temperatures and with approximately the same intensity as for the catalyst that has worked for 75 h.

To find out the limit of thermal stability of the catalyst in the reaction medium, a series of experiments with increasing the temperature in the reactor to specified values, at which the sample was kept for 1 h, after which the temperature was reduced to the reference and the activity, was reduced. As the results showed, regardless of the method of preparation of the catalyst, increasing its temperature to 430 ˚C did not affect its properties, the activity in the oxidation of methacrolein at this temperature after each successive increase in its temperature remained the same. Higher temperature (430 ˚C) causes irreversible loss of activity and selectivity (4 and 5–6 times, respectively).

To clarify this phenomenon, radiographic, infrared spectroscopic and thermographic analyses of samples before and after their heating were carried out.

On the X-ray film of the sample heated under reaction conditions at 405 ˚C and losing its activity, a sharp decrease in the intensity of reflexes characteristic of the ammonium salt of 12-Mo-P-acid and the appearance of new reflection maxima close to the structure of rhombic MoO, possibly somewhat distorted (Fig. 4).

The loss of activity of the catalyst worked under reaction conditions at t > 430 ˚C is associated with the destruction of the active phase of the heteropolymer catalyst (Keggin cell) and the formation of inactive $MoO_3$.

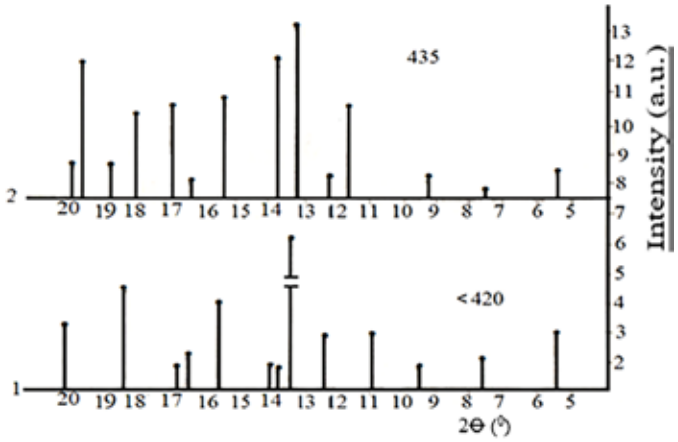


Figure 4. X-ray diffraction of the catalyst sample: 1 – after heating at t = 420 ˚C; 2 – after heating at t = 435˚C; * – reflection indices for HPS; * – for $MoC_3$

The process of decomposition of HPC obviously occurs according to the equation:

$$(NH_4)_{3-7}\ Me_7PMO_{12}O_{40} \cdot n\ H_2O \rightarrow MoO_3 + NH_3 + + MeMoO_4 + P_2O_5 + H_2O$$

It should be noted that the decomposition temperature of the studied catalyst is higher (~ by 60 ˚C) than that of phosphormolybdenum acid (370 ˚C), which is used as an industrial catalyst for methacrolein oxi-

dation. It can be assumed that an increase in thermal stability of investigated samples is achieved due to the modification of $H_3PMo_{12}O_{40}$ by different additives.

In, it was shown that $NH_3$ from the gas phase is strongly adsorbed on the HPA-catalysts, blocking the conversion centers of methacrolein, whereas $NH_4^+$-groups in the catalyst structure has little effect on its activity. It can be assumed that the activation of the catalyst that has worked for 35–40 h is associated with the removal of such firmly adsorbed ammonia and the release of the active centers of the ammonia surface. This leads to a significant increase in the activity of the catalyst (conversion of methacrolein increases more than 2-fold). At the same time, there is only a slight decrease in its ammonium content. This opens the possibility of purposefully changing the structure of the catalyst in one way or another to improve its catalytic properties.

**References:**


1. Staroverova I. N., Kutyrev M. Yu., Khvtisiashvili L. G. Antioxidant Activity of Methano- and Cyclopentenofullerenes. Kinetics and catalysis,– M.,– Vol. 27.– No. 3. 1986.– P. 691–697. (in Russian).
2. Sergienko V. S., Detusheva L. G., Yurchenko E. N., Poray-Koshits M. A. Effect of Fullerene Containing a Maleopimarimide Substituent on the Kinetics of Liquid-Phase Radical Chain Oxidation of Ethylbenzene. Journal of Structural Chemistry.– V. 22.– No. 6. 1981.– P. 38–42. (in Russian)
3. Tillaeva S. F., Sattorov M. O. Study of the quality of oil products modified for catalysts, "Science and Education", – Bukhara. 2022. – No. 3.– P. 123–130. (in Uzbekistan).
4. Mirzaliev S. S., Yaminov F. F. Influence of modifying factors on the environment and active centers of catalysts, Engineering and Technical Institute.–Bukhara. 2016.– P. 38–45. (in Uzbekistan).
5. Staroverova I. N., Kutyrev M. Yu. IY All-Union conference on the mechanism of catalytic reactions. Conversion of volatile organic compounds on platinum and metal oxide catalysts.– M.,– No. 2. 1986.– P. 43–46. (in Russian).
6. Sennerich M., Weidler P. Hexagonal Mo/V/W mixed oxide as a catalyst for the partial oxidation of methacrolein to methacrylic acid. Catal. Commun. 2020.– 141 p. URL: https://doi.org/10.1016/j.catcom.2020.106016
7. Krauw K. Entwicklung und Einsatz einer DRIFTS-Meßzelle zur In-Situ-Spektroskopie Heterogen Katalysierter Gasphasenoxidationen; Technische Universität Darmstadt: Darmstadt. 2000.– P. 235–249. (in Germany).
8. Xue J., Yin H., Li H., Zhang D., Jiang T., Yu L., Shen Y. Oxidation of cyclopentene catalyzed by tungsten-substituted molybdophosphoric acids. Korean Journal of Chemical Engineering.– V. 26.– No. 3. 2009.– P. 654–659. (in Korean).
9. Védrine J. C. Metal Oxides in Heterogeneous Oxidation Catalysis: State of the Art and Challenges for a More Sustainable World. ChemSusChem No. 12. 2019.– P. 577–588. DOI: 10.1002/cssc.201801974.
10. Darabi M. J., Dubois J. L., Cavani F., Rostamizadeh M., Patience G. S. Catalysis for the synthesis of methacrylic acid and methyl methacrylate. Chemical Society Reviews. 2018.– P. 7703–7738. URL: https://doi.org/10.1039/D2CS00779G
11. Nagai K., Ui T. Trends and Future of Monomer–MMA Technologies. Sumitomo Chem.– No. 2. 2004.– P. 4–13. (in Japan).
12. Belousova A. S., Esipovicha A. L., Otopkova K. V. Investigation of the process of vapor-phase dehydration of glycerol to acroleiin in the presence of polyoxometallates Kinetics and catalysis.– V. 61.– No. 4. 2021.– P. 541–548. URL: https://doi.org/10.1002/jctb.4273

13. Lowell S., Shields J. E., Thomas M. A., Thommes M. Characterization of Porous Materials and Powders: Surface Area, Pore Size and Density. Netherlands: Springer, 2020.– 350 p. DOI:10.1007/978-1-4020-2303-3
14. Danov S. M., Esipovich A. L., Belousov A. S., Rogozhin A. E. Effect of Diethylene Glycol on the Formation of the Oxide Precursor of the Nickel–Molybdenum Hydrotreating Catalyst. Russian Journal Applied Chemistry.– V. 87. 2019.– P. 461–469. (in Russian).
15. Belousov A. S., Rogozhin A. E. Investigation of the process of vapor-phase dehydration of glycerol to acroleiin in the presence of polyoxometallates. Kinetics and catalysis.– Vol. 61.– No. 4. 2020.– P. 541–548. DOI: 10.31857/S0453881120030077
16. Thanasilp S., Schwank J. W., Meeyoo V., Pengpanich S., Hunsom M. Comparison of citric acid and glycol effects on the state of active phase species and catalytic properties of CoPMo/Al2O3 hydrotreating catalysts. Journal of Molecular Catalisis A- Chem.– V. 380. 2018.– P. 67–68. DOI: 10.1016/j.mcat.2018.05.020
17. Liu R., Wang T., Liu C., Jin Y. Biomass valorisation over polyoxometalate-based catalysts Chin. J. Catal.– V. 34. 2021.– P. 2174. DOI: 10.1039/D0GC03190 A
18. Abdullayeva M. Y., Habibov I. A. Improvement of the electrical properties of synthetic liquid dielectric for pulse capacitors. EUREKA, Physics and Engineeringthis link is disabled. 2020.– P. 13–18.
19. Guseynova E. B., Mustafayeva R. E. Modification and study by the method of planning an experiment of a tin-antimony catalyst for the gas-phase oxidation of isobutylene to methacrolein. Natural and mathematical sciences in the modern world. Novosibirsk 2015.– P. 73–83. (in Russian).
20. Dong D. Q., Yang S. H., Wu P., Wang J. Z., Min L. H., et al. Copper-Catalyzed Difluoroalkylation Reaction. Molecules – 27. 2022.– P. 84–61. URL: https://doi.org/10.3390/ molecules 27238461

**https://doi.org/10.29013/AJT-23-5.6-36-43**

*Erkayeva Nazokat Aktamovna,*
*Doctoral student of Tashkent Institute of Chemical Technology.*
*Erkayev Aktam Ulashevich,*
*Doctor of technical sciences,*
*Professor, Tashkent Institute of Chemical Technology*
*Kaipbergenov Atabek Tulepbergenovich,*
*Doctor of technical sciences,*
*Professor, Director of the Nukus Mining Institute,*
*Kucharov Bahrom Xayriyevich,*
*Doctor of technical sciences,*
*Institute of General and Inorganic Chemistry.*
*Reimov Karjawbay Dauletbaevich,*
*doctor of technical sciences (PhD),*
*associate professor, of Ajiniyaz Institute*

# INFLUENCE OF THE COMPOSITION ON THE RHEOLOGICAL AND FUNCTIONAL PROPERTIES OF THE COMPOSITION OF LIQUID SYNTHETIC DETERGENTS

**Abstract.** The optimal conditions for production of synthetic detergents. On the basis of products and local raw materials recommended different formulations of synthetic cleansers.

**Keywords:** cleaning products, surfactants, sodium hydroxide, sodium carbonate, foaming, corrosion.

The problem of cleaning arises in the most various branches of a national economy that testifies to relevance of this problem.

Efficiency of detergent and quality of cleaning of a metal surface considerably depends on properties of the processed surface – its roughness, sensitivity to corrosive attack of detergent, existence to surfaces of oxides, its uniformity.

The accelerated development of chemical industry allowed to expand in recent years considerably the range of domestic synthetic detergents (SD) and to increase their production.

The analysis of the let-out SD shows that water solutions of the surface-active substances (SAS) and their composition with active additives are more and more applied to degreasing of various surfaces instead of alkalis. Preparations like emulsions and other two-phase systems are practically absent.

Development of production of SD in us in the country has to be directed on creation of alkaline detergents which allow to exclude use of flammable and toxic solvents.

When studying the dependence of the rheological properties of SD, mixtures were prepared that included potassium carbonate, sodium hydroxide, sodium carboxymethyl cellulose (SCC), Trilon B, liquid glass, monoammonium phosphate (MAP), sodium laureth sulfate (SLES), linear alkyl benzene sulfate (LABSA) and water. The initial components were displaced at a temperature of 60 °C and various mass ratios (Table 1).

Table 1.– Mass ratios of the reacting components used for the preparation of SD*

| № | $K_2CO_3$ | NaOH | Trilon B,% | Liquid glass | MAP,% | SLES,% | LABSA,% |
|---|---|---|---|---|---|---|---|
| 1 | 1.896 | 0.481 | 2.0 | 0.856 | 2.0 | 10.0 | 4.0 |
| 2 | 1.871 | 0.484 | 2.0 | 0.846 | 2.0 | 5.0 | 2.0 |
| 3 | 1.870 | 0.484 | 2.0 | 0.846 | – | 5.0 | 2.0 |
| 4 | 1.851 | 0.478 | – | 0.837 | 2.0 | 5.0 | 2.0 |
| 5 | 1.860 | 0.479 | – | 1.178 | – | 5.0 | 2.0 |
| 6 | 1.871 | 0.481 | – | 1.184 | – | 10.0 | 4.0 |
| 7 | 3.450 | 2.550 | 1.0 | 0.836 | 1.0 | 5.0 | 2.0 |
| 8 | 3.460 | 2.560 | – | 1.207 | – | 5.0 | 2.0 |

**When receiving the first batch of samples, SLES was used, and the second batch was LABSA*

Samples of the samples belonging to the first batch were synthesized in the presence of SLES, and those of the second batch were synthesized in the presence of LABSA. The composition of samples from batch 1 is significantly different from the composition of the original components. For example, samples 1 and 6 contain twice as much SLES. Sample 3, compared to sample 1, contains less SLES and is characterized by the complete absence of MAP. Samples No. 4–6 contain a relatively large amount of liquid glass, while Trilon B and MAP are absent at all. Samples 7 and 8 contain more and less potassium carbonate and sodium hydroxide, respectively.

Sample samples from Lot 2 differ from Lot 1 in the absence of sodium laureth sulfate. The content of potassium carbonate and sodium hydroxide is in the range of 10.00–18.65% and 8–15%. The content of SD is 1%, which remains unchanged. Similarly, to the sample of batch 1 in batch 2, the amount of liquid glass and MAP varies in the range of 10–12 and 1–2%, respectively.

Experimental data (Table 2) dependence of the density of the samples on the mass ratio of the initial components showed that at a synthesis temperature of 20%, sample 1 has the maximum density when containing a relatively large amount of sodium laureth sulfate. Sample 5, unlike sample 4, does not contain Trilon B and MAP. In contrast to the sample and with a density of 1.2705 g/cm$^3$, in sample 5, in the absence of Trilon B, the density of the suspension increases to 1.2847 g/cm$^3$. In this case, it is also necessary to take into account the presence of liquid glass, which contributes to an increase in the density of the sample. Despite the fact that sample 6 contains more water glass than sample 7, its density increases to a value of 1.2900 g/cm$^3$. Although Trilon B and monoammonium phosphate are absent in sample compared to sample 7, their densities practically do not differ from each other.

The data of Table 2 show that the presence of LABSA in synthetic detergents leads to a decrease in the density of the samples to 1.281 g/cm$^3$ (Table 2).

Table 2.– The dependence of the density of the synthesized SD on the mass ratio of the initial components and temperature

| № | Temperature, °C (batch 1) | | | Temperature, °C (batch 1) | | |
|---|---|---|---|---|---|---|
| | 20 | 40 | 60 | 20 | 40 | 60 |
| *1* | *2* | *3* | *4* | *5* | *6* | *7* |
| 1 | 1.305 | 1.192 | 1.160 | 1.281 | 1.270 | 1.263 |
| 2 | 1.290 | 1.233 | 1.240 | 1.284 | 1.270 | 1.265 |
| 3 | 1.290 | 1.278 | 1.266 | 1.274 | 1.266 | 1.256 |
| 4 | 1.271 | 1.272 | 1.258 | 1.280 | 1.272 | 1.265 |

| *1* | *2* | *3* | *4* | *5* | *6* | *7* |
|---|---|---|---|---|---|---|
| 5 | 1.285 | 1.265 | 1.213 | 1.280 | 1.278 | 1.270 |
| 6 | 1.290 | 1.264 | 1.267 | 1.287 | 1.276 | 1.266 |
| 7 | 1.275 | 1.248 | 1.271 | 1.256 | 1.248 | 1.236 |
| 8 | 1.280 | 1.270 | 1.256 | 1.286 | 1.262 | 1.259 |

Experimental data show that the content of sodium laureth sulfate has the greatest effect on the density of the synthesized SD.

It was also found that with an increase in temperature from 20 °C to 60 °C, the density values of SD samples decrease. For example, the density of sample No. 2 at a temperature of 20 °C is 1.290 g/cm$^3$, and with an increase in temperature to 60 °C, the density of the sample decreases sharply to a value of 1.160 g/cm$^3$. A similar pattern is observed for other samples.

An increase in temperature also lowered the values of the viscosity of the SD in the temperature range of 20–60 °C (Table 3). The table shows that, for example, sample No. 2 from the first batch at a temperature of 20 °C has a viscosity of 157.61 cPs. A similar pattern is observed for the SD samples from the second batch, where at 20 °C sample No. 2 shows a viscosity value of 162.65 cPs, and at 60 °C12.04 cPs.

Table 3.– The dependence of the viscosity of the obtained SD on the composition of the initial mixture and temperature

| № | Temperature, °C (batch 1) | | | Temperature, °C (batch 1) | | |
|---|---|---|---|---|---|---|
| | **20** | **40** | **60** | **20** | **40** | **60** |
| 1 | 95.63 | 32.87 | 11.90 | 140.63 | 37.75 | 11.93 |
| 2 | 157.61 | 63.14 | 16.11 | 162.65 | 43.85 | 12.04 |
| 3 | 159.66 | 48.82 | 15.58 | 132.45 | 35.72 | 13.50 |
| 4 | 157.24 | 51.09 | 14.04 | 169.88 | 49.47 | 13.47 |
| 5 | 268.20 | 42.31 | 17.54 | 141.25 | 35.39 | 10.57 |
| 6 | 110.11 | 37.42 | 10.00 | 163.27 | 42.87 | 19.93 |
| 7 | 283.29 | 87.87 | 35.76 | 180.73 | 53.04 | 20.80 |
| 8 | 190.49 | 61.18 | 20.72 | 117.03 | 41.00 | 12.64 |

The composition of the original components also has a significant impact on the viscosity values. According to the chemical analysis in sample 1, compared to sample 2, it contains a relatively large amount of sodium laureth sulfate, as a result of which the viscosity value of this sample decreases. This proves that sodium laureth sulfate reduces the viscosity of the obtained SD. Unlike the others, sample 5 contains a relatively large amount of liquid glass, and the viscosity of this sample at 20 °C is 268.20 cPs, which is significantly higher than in plugs 1–4. Sample 7 is high in potassium carbonate and therefore has a higher viscosity than samples 1–6.

And in sample 6 there is less potassium carbonate and more alkali than in sample 8, i.e. according to the viscosity values, the alkali increases the viscosity of the SD samples.

When analyzing the viscosity values of samples of batch 2, it was revealed that these indicators at 20 °C change in the range from 117.03 to 180.74 cPs. The minimum viscosity value of 117.032 cPs is typical for sample 8, which contains the lowest alkali content and lacks Trilon B. With a decrease in temperature in the SD samples of lot 2, the viscosity value also sharply decreased with decreasing temperature. For example, at a temperature of 20 °C, the viscosity of sample 1 is 140.63 cPs, and with an

increase in temperature to 40 °C, this value decreases by a factor of 3.72.

To study the dependence of the rheological properties of SD samples on temperature and concentration in the laboratory, various concentrations were prepared in the laboratory conditions, solutions of the obtained SD were prepared at different concentrations (Tables 4 and 5).

Table 4. – Dependence of SD density on temperature and concentration

| № | Solution, C% | Temperature, °C (batch 1) | | | Temperature, °C (batch 1) | | |
|---|---|---|---|---|---|---|---|
| | | 20 | 40 | 60 | 20 | 40 | 60 |
| 1.1 | 0.5 | 1.001 | 0.994 | 0.98 | 1.00 | 0.99 | 0.98 |
| 1.2 | 1.0 | 1.004 | 0.997 | 0.99 | 1.00 | 0.99 | 0.99 |
| 1.3 | 2.0 | 1.007 | 1.000 | 0.99 | 1.00 | 0.99 | 0.99 |
| 1.4 | 5.0 | 1.015 | 1.010 | 1.00 | 1.01 | 1.00 | 0.99 |
| 1.5 | 10.0 | 1.027 | 1.022 | 1.01 | 1.02 | 1.01 | 1.00 |
| 2.1 | 0.5 | 1.001 | 0.994 | 0.98 | 1.00 | 0.99 | 0.98 |

Table data 4 show that at 20 °C a 0.5% solution has a density value of 1.001g/cm$^3$. With an increase in temperature to 60 °C, the density value decreases to 0.99 g/cm$^3$. Increasing the concentration of solution 1 to 10% increases the density of the sample to 1.0272 g/cm$^3$. An increase in the concentration of the solution leads to an increase in the density values. A similar pattern is typical for all SD samples. With an increase in the 0.5% concentration of sample 6 at a temperature of 20 °C to 10%, the density of the solution from 1.06 increases to a value of 1.037 g/cm$^3$.

Table 5. – Dependence of SD viscosity on concentration and temperature

| № | Solution,% | Temperature, °C (batch 1) | | | Temperature, °C (batch 1) | | |
|---|---|---|---|---|---|---|---|
| | | 20 | 40 | 60 | 20 | 40 | 60 |
| 1 | 0.5 | 13.90 | 5.77 | 2.39 | 13.20 | 6.18 | 2.47 |
| 2 | 1.0 | 14.63 | 6.10 | 2.57 | 13.84 | 6.43 | 2.54 |
| 3 | 2.0 | 15.42 | 6.43 | 2.70 | 15.26 | 6.83 | 2.86 |
| 4 | 5.0 | 16.04 | 6.75 | 2.86 | 16.21 | 6.92 | 2.93 |
| 5 | 10.0 | 17.30 | 6.83 | 2.90 | 17.30 | 7.57 | 3.18 |

With an increase in the concentration of the solution, its viscosity increases, and this creates difficulties in pumping the solution within the workshop or enterprise. As an example, we can cite the fact of an increase to 17.31 cPs in the viscosity of a solution of 13.9 cPs at a concentration and temperature of 10% and 20 °C, respectively. This is a pattern characteristic of other SD samples. The experimental data of Table 5 show that the samples are practically characterized by the same temperature and concentration, identical viscosity.

To study the effect of SD concentration on pH, solutions of various SD concentrations from the first batch were prepared.

Table 6. – The dependence of pH SD on the concentration of the solution

| Solution,% | SD sample numbers from the first batch | | | | | | | |
|---|---|---|---|---|---|---|---|---|
| | 1 | 2 | 3 | 4 | 5 | 6 | 7 | 8 |
| *1* | *2* | *3* | *4* | *5* | *6* | *7* | *8* | *9* |
| 0.5 | 10.50 | 10.51 | 10.61 | 10.70 | 10.50 | 10.71 | 10.20 | 10.70 |
| 1 | 10.65 | 10.61 | 10.70 | 10.81 | 10.61 | 10.80 | 10.40 | 10.80 |
| 2 | 10.70 | 10.72 | 10.81 | 10.91 | 10.71 | 10.92 | 10.71 | 10.91 |

| *1* | *2* | *3* | *4* | *5* | *6* | *7* | *8* | *9* |
|---|---|---|---|---|---|---|---|---|
| 5 | 10.81 | 10.80 | 10.90 | 11.10 | 10.80 | 10.41 | 10.71 | 11.22 |
| 10 | 10.90 | 10.91 | 11.01 | 11.10 | 10.90 | 11.10 | 10.70 | 11.30 |

The data obtained allow us to state that with an increase in the concentration of SD, the pH index increases, which ranges from 10.2 to 11.3. The maximum pH value of the solution is observed in sample 8 with a concentration of 10%. This sample contains an increased amount of potassium carbonate, sodium laureth sulfate and less alkali. Although sample 1 contains an increased amount of sodium laureth sulfate, sample 3 does not contain MAP, and samples 1–3 contain identical amounts of alkali and potassium carbonate, the pH value of the solution varies in the range of 10.5–10.9. Increasing the amount of liquid in sample 5 lowered the pH value.

Next, laboratory experiments were performed to study the foaming ability of SD depending on the ratio of the initial components (Fig. 1 and 2).

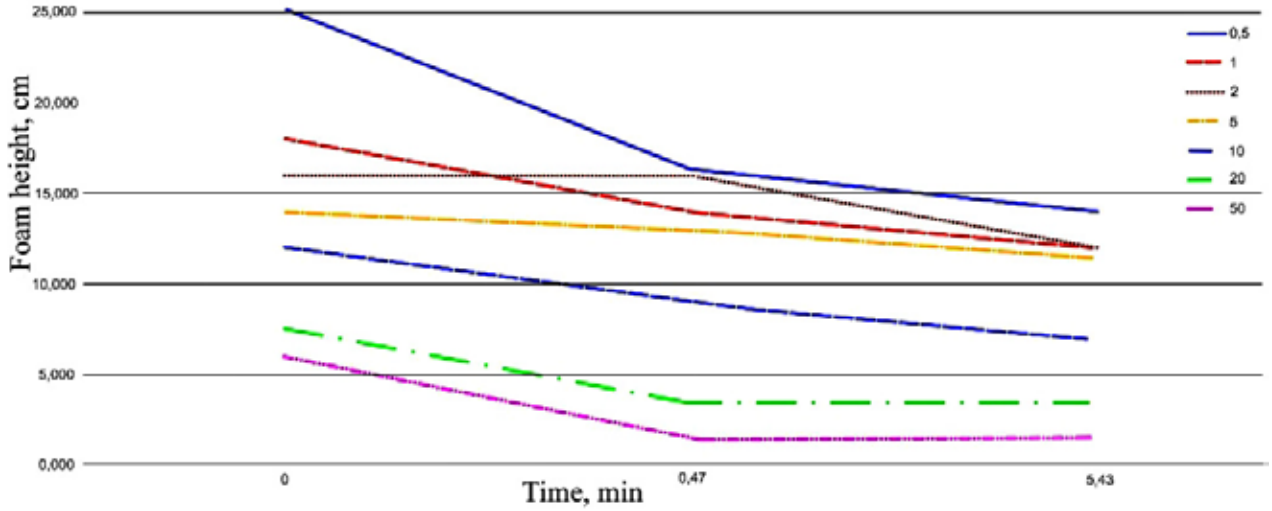


Figure 1. Effect of SD concentration on foaming (1 batch, 1 sample)

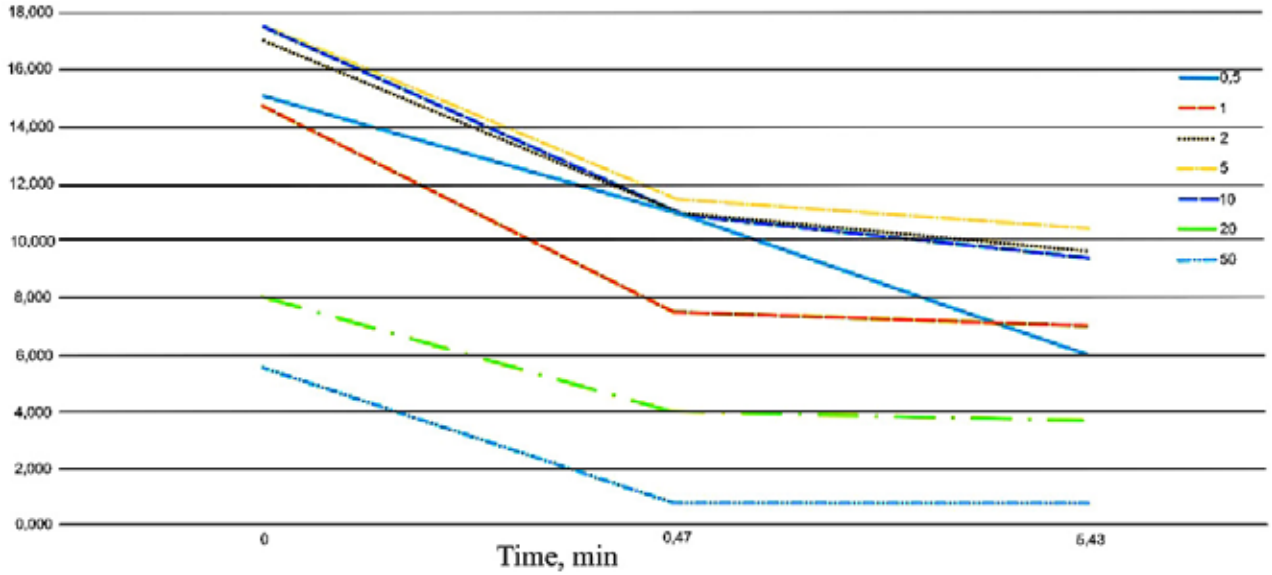


Figure 2. Effect of SD concentration on foaming (1 batch, 5 sample)

As the data in Fig. 1 show, solutions with different ratios of reagents have different foaming abilities. For example, sample 1, which has sodium laureth sulfate in its composition than sample 2, has a greater foaming ability. A solution of this sample at a concentration of 0.5% in the initial period of time forms a foam 25 cm high, while sample 2 at the same concentration forms a foam 9 cm high.

Sample 1 showed high foam resistance, a foam 5 cm high was recorded for 2 days. Sample 2 foam was less stable, since even at a high solution concentration of 5–10%, the foam height was 5 and 10 cm, respectively.

Sample 6 also contains a large amount of sodium laureth sulfate, which forms the maximum foam height in the initial period. The absence of MAP in the samples contributed to an increase in foaming ability.

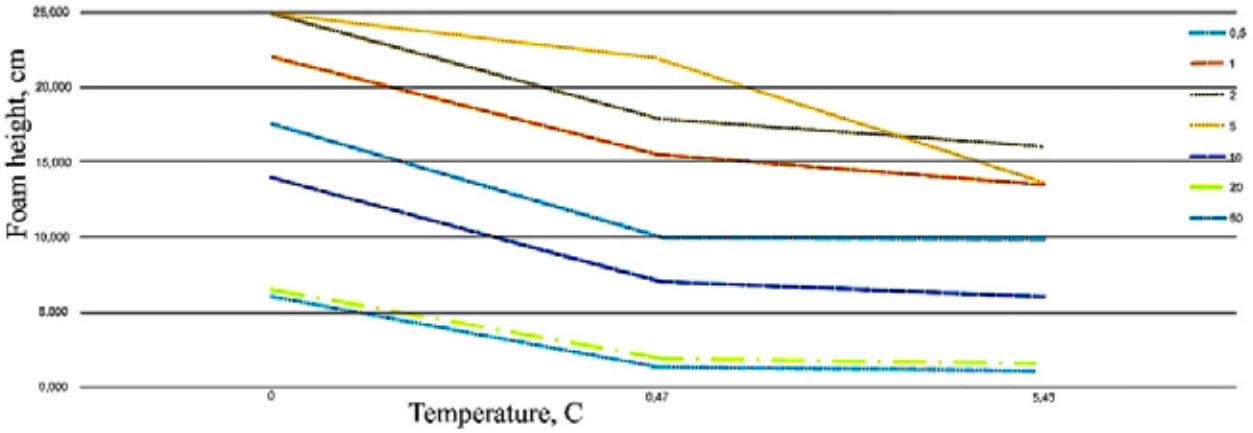


Figure 3. Effect of SD concentration on foaming (batch 2, sample-1)

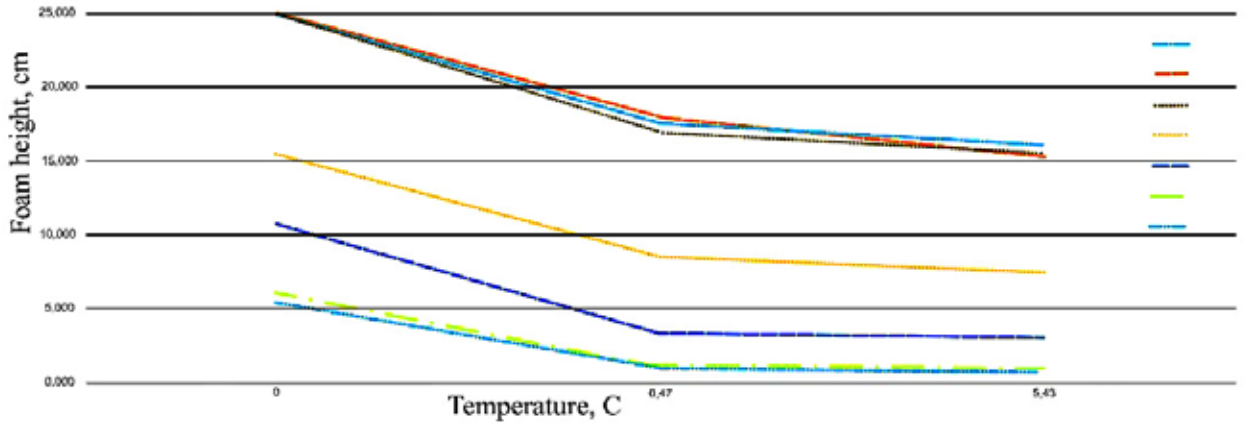


Figure 4. Effect of SD concentration on foaming (batch 2, sample-5)

Experimental data showed that the maximum foam height at the beginning of the process occurs in solutions with a concentration of 1.2% and is 25 cm. In this sample, at the beginning of the process, a foam 25 cm high is formed. Containing in its composition the largest amount of LABSA and liquid glass 0.5; 1; 2; 5% concentration of sample 6 in the initial period of the process formed a large height of stable foam (25 cm).

Due to the above, the technological process of production is simplified and makes it possible to significantly reduce material and energy costs.

Subsequently, solutions of all samples were prepared with a concentration of 0.5; 1 and 2% to study their washing ability.

The results of the research showed that the 2% solution of sample 1 (sample 1.3) had the highest

washing power (48%), and sample 1 of 0.5% concentration had the lowest washing power (20%).

It was found that with an increase in the concentration of the drug from 0.5% to 0.2%, the washing ability increases. For example, sample 2 with a solution concentration of 0.5% has a washing power of 34%. With an increase in concentration to 2%, the washing ability increases to 38% (sample 2.3).

It should be noted that in sample 4.1, the washing power is 24%. At a solution concentration of 2%, a sharp increase in washing power up to 38% is observed (Tables 7 and 8).

Table 7.– The dependence of the washing power of SD concentration (samples from lot 1)*

| Sample no. | 1.1 | 1.2 | 1.3 | 2.1 | 2.2 | 2.3 |
|---|---|---|---|---|---|---|
| Washing capacity,% | 54 | 60 | 62 | 54 | 56 | 58 |
| Sample no. | 3.1 | 3.2 | 3.3 | 4.1 | 4.2 | 4.3 |
| Washing capacity,% | 58 | 58 | 68 | 44 | 46 | 58 |
| Sample no. | 5.1 | 5.2 | 5.3 | 6.1 | 6.2 | 6.3 |
| Washing capacity,% | 42 | 44 | 44 | 44 | 46 | 48 |
| Sample no. | 7.1 | 7.2 | 7.3 | 8.1 | 8.2 | 8.3 |
| Washing capacity,% | 40 | 41 | 54 | 56 | 58 | 60 |

** – numbers of samples correspond to the numbers of samples in Table 6*

The results of the studies (Table 7) indicate that prepared in the presence of LABSA in SD have a greater detergency than samples of SD obtained in the presence of sodium laureth sulfate. The maximum washing power in these samples was 90%.

Solutions with a concentration of 5% had the best washing ability. For example, a 0.5% solution of the first sample had a washing power of 60%, while in a 5% solution it was 74%. In the absence of Trilon B in sample 4, depending on the concentration, a different change in washing ability was obtained. This sample at a 0.5% solution concentration has a detergency of 58%, and at a concentration of 2%, the detergency reached 72%, which is 14% higher than the detergency value of a 0.5% solution.

Table 8.– The dependence of the cleaning power of SD on the concentration (samples from batch 2) *

| Sample no. | 1.1 | 1.2 | 1.3 | 2.1 | 2.2 | 2.3 |
|---|---|---|---|---|---|---|
| Washing capacity,% | 60 | 74 | 74 | 70 | 64 | 76 |
| Sample no. | 3.1 | 3.2 | 3.3 | 4.1 | 4.2 | 4.3 |
| Washing capacity,% | 60 | 64 | 74 | 58 | 78 | 72 |
| Sample no. | 5.1 | 5.2 | 5.3 | 6.1 | 6.2 | 6.3 |
| Washing capacity,% | 80 | 82 | 80 | 84 | 88 | 90 |
| Sample no. | 7.1 | 7.2 | 7.3 | 8.1 | 8.2 | 8.3 |
| Washing capacity,% | 52 | 54 | 56 | 58 | 60 | 72 |

** – numbers of samples correspond to the numbers of samples in Table 4*

According to Table 8, sample 6 with a concentration of 2% has the highest detergency. This sample contains a small amount of LABSA in the absence of Trilon B and MAP.

The results of the conducted studies allow us to conclude that with a change in temperature and mass ratios of compounds, it has a significant effect on the density of SD.

A study of the dependence of the foaming ability of SD on the mass ratio of the reacting components showed this solution to have a significant effect on foaming, and the samples differ significantly in this feature.

In the sample containing the largest amount of sodium laureth sulfate, the maximum detergency is observed. In addition, it was found that the samples in the absence of MAP and Trilon B additives also have the best washing ability.

**References:**


1. Ветошкин Ю. С. Прогнозирование производства и потребления СМС и товаров бытовой химии в России до 2010 г. / Бытовая химия.– № 25. 2007.– 16 с.
2. Anders E. K. Глобальный и Российский рынок СМС. Состояние, развитее, перспективы / Бытовая химия.– № 26. 2007.– 5 с.
3. Бухштаб З. И. Технология синтетических моющих средств / З. И. Бухштаб, А. П. Мельник, В. М. Ковалёв.– М.: Легпромбытиздат, 1988.– 320 с. ISBN5-7088-0365-7
4. Николаев П. В., Петрова Н. А. Основы химии и технология производства синтетических моющих средств.– Иваново, 2007.–405 с.
5. Эркаева Н. А., Шарипова Х. Т., Каипбергенов А. Т., Эркаев А. У., Кучаров Б. Х. Влияние состава моющих композиций на их функциональные показатели. Узбекский химический журнал, – № 3.2019. – С. 76–83.
6. Kaipbergenov A. T., Erkaev A. U., Shadmanov O. Ya., Tairov Z. K. Development of compounding powder cleaners.– Austrian Journal of Technical and Natural Sciences,– № 11–12. 2015.– P. 56–57.
7. Эркаева Н. А., Эркаев А. У., Каипбергенов А. Т. Физико-химические и товарные свойства синтетических моющих средств, полученных на основе сесквикарбоната натрия.– Universum: технические науки,– № 7.– 3(76). 2020.– С. 61–65.
8. Erkayeva N. A., Erkayev A. U., Nurmurodov T. I., Kaipbergenov A. T. A study on the influence of synthetic compositions of liquid detergents on rheological and functional properties.– Chemical Technology, Control and Management,– № 4. 2019.– P. 53–61.

# Contents